Accounting for Time in Life Cycle Assessment: Case Study of a Mass Timber Building

By Lihan Jin

Faculty of Applied Science and Engineering

Supervisor: Professor Ted J. Kesik

John H. Daniels Faculty of Architecture, Landscape, and Design

April 14th, 2022

B.A.Sc. Thesis

Division of Engineering Science
UNIVERSITY OF TORONTO

Abstract

Due to the rising popularity of mass timber buildings, it is crucial to critically examine the impact that wooden construction has on the climate. Unfortunately, the climate impact of wood is highly contested due to a knowledge gap in how to account for time in life-cycle assessment (LCA). The traditional LCA approach of giving equal weight to time is unreasonable because in general, the climate impact of a carbon flow depends on its time of occurrence. This thesis proposes an 'advanced' LCA method that incorporates the dimension of time. The proposed method employs the absolute global temperature change potential (AGTP), and uses simple emission functions to model the emission profiles of buildings. A sensitivity analysis conducted using the proposed method discovered that the AGTP of a mass timber building both depends on the rotation period of the forest stand from which raw materials were extracted, and on the assessment time horizon. It highlights the need for advanced LCA methods by showing the inability of traditional LCA to capture the natural evolution of climate impacts over time. Overall, due to its simplicity, this thesis recommends the proposed method for inclusion in LCA standards and for use by building designers to compare the climate impacts of material and design decisions at the early stages of a building project. It is hoped that future research will further the standardization of an LCA method that accounts for time, and create a more complete understanding of the climate implications of the shift to mass timber.

Acknowledgements

This thesis marks the home stretch of my 6-year adventure through Engineering Science. Though it is my honest and original work, the accomplishment would not have been possible without the unparalleled support of several people whom I'd like to deeply thank. It is only with their advice and encouragement that I was not only able to face what at first seemed to be an insurmountable challenge, but to emerge from the other side as a changed individual.

Professor Ted J. Kesik, my thesis supervisor,
For providing insightful advice and guidance on my research, and
For helping me find meaning in my work, and the motivation to finish it well.

My parents, Dongmei Yang and Zhonglei Jin,
For bringing me to this wonderful country and enriching learning environment,
For instilling in me a culture of hard work and perseverance, and
For constantly believing in me, even when challenges ahead seemed unconquerable.

Table of Contents

List of Figures **v**

List of Tables **vii**

1 Introduction **1**

2 Literature Review **7**

2.1 Traditional LCA Methods 7

2.2 Advanced LCA Methods 9

2.2.1 Moura-Costa Method 11

2.2.2 Lashof Method 13

2.2.3 Dynamic LCA 15

2.2.4 GWP_{bio} Method 17

2.3 Summary of Literature Review 22

3 Proposed LCA Method **23**

3.1 Differences from the GWP_{bio} Method 23

3.1.1 Use of Multiple 'Emission Functions' 23

3.1.2 Decoupling of Emissions from Forest Growth 24

3.1.3 Absolute Global Temperature Change Potential 26

3.2 Derivation of Characterization Factors 28

3.3 General Procedure 31

4 Sensitivity Analysis Using the Proposed LCA Method **32**

4.1 Objectives of the Analysis 32

4.2 Description of the Case Study Building 33

4.3 LCA Scope 34

4.4 Variables of Interest 35

4.4.1 Assessment Time Horizon 35

4.4.2 Forest Rotation Period 35

4.5 Control Variables 39
4.5.1 Building Lifetime 39
4.5.2 Residue and Waste Treatment Scenarios 39
4.6 Methodology 41
5 Results 43
5.1 Climate Impacts of Unit Emissions and Sequestrations 43
5.2 Results of the Sensitivity Analysis 47
5.2.1 Scenario Analysis 47
5.2.2 Comparison with the Original Study 51
6 Discussion 53
6.1 General Remarks 53
6.2 Strengths and Weaknesses of the Proposed Method 54
6.3 Practicality of the Proposed LCA Method for Standardization 55
7 Conclusion 58
References 60
Appendix A AGTP Factors for Unit Emissions and Sequestrations 67
Appendix B Specific LCA Procedure for Mass Timber Buildings 71
Appendix C Sample Calculation Using the Proposed LCA Method 76
Appendix D Derivation of Material Efficiencies 80

List of Figures

Figure 1	Embodied carbon, both absolute and relative to total life cycle emissions, of buildings built to various performance standards.	1
Figure 2	Evolution of the carbon footprint of a wood product over time.	3
Figure 3	Embodied carbon reduction potential versus phase of a building project.	6
Figure 4	Inconsistency in the overall assessment time horizon of an LCA study due to use of a time-independent characterization factor, the 100-year GWP.	9
Figure 5	Comparison of GWP results for wood building LCAs using traditional and advanced (dynamic) LCA methods.	10
Figure 6	The concept of equivalence between carbon storage and avoided fossil emissions.	12
Figure 7	The benefit of carbon storage viewed as delaying the radiative forcing caused by an emission beyond the assessment time horizon.	14
Figure 8	Carbon flux system upon the original GWP_{bio} method was developed.	17
Figure 9	PDFs used to represent distributed bioCO_2 emissions.	19
Figure 10	Decomposing a complex emission profile into simple emission functions.	24
Figure 11	Deviation of an emission profile from the one assumed by GWP_{bio} due to delayed emissions relative to carbon sequestration by forest growth.	25
Figure 12	'Cause and effect chain' of the impacts arising from a GHG emission.	27
Figure 13	The three emission functions investigated in the present study.	30
Figure 14	General procedure of the proposed LCA method.	31
Figure 15	Structural model of the case study building	33
Figure 16	Example of a multi-cohort age structure of a forest stand, illustrating complexity in defining the forest rotation period.	36
Figure 17	Cumulative forest growth functions created using the Schnute model for rotation periods of 25, 75, and 200 years.	37
Figure 18	Growth rate-versus-time graphs created using the Schnute model for rotation periods of 25, 75, and 200 years.	38

Figure 19 The 12 scenarios, representing all possible combinations of assessment time horizon and forest rotation period, used in the sensitivity analysis. 38

Figure 20 AGTP versus time graph and radiative forcing profile of a 1 kg pulse CO_2 emission. 44

Figure 21 AGTP versus time graph and radiative forcing profile of a 1 kg pulse CH_4 emission. 44

Figure 22 AGTP versus time graphs of 1 kg distributed CO_2 emissions following the negative exponential emission function (equation 14), for various values of τ. 45

Figure 23 AGTP versus time graphs of 1 kg distributed CH_4 emissions following the negative exponential emission function (equation 14), for various values of τ. 46

Figure 24 AGTP versus time graphs of 1 kg CO_2 removals by forest growth modeled using the Schnute growth function for various forest rotation periods, *r*. 47

Figure 25 AGTP of the case study building at time horizons of 28, 78, 128, and 178 years for forest rotation periods of 25, 75, and 200 years. 48

Figure 26 AGTP-versus-time graphs of the case study building under 3 forest growth cases, as well as of the 4 main life cycle stages included in the LCA: MTC, residue treatment, end-of-life waste treatment, and forest growth. 50

Figure 27 AGTP of the case study building under the 12 analysis scenarios compared to the result of the original study by Chen et al. (2020) [35] 51

List of Tables

Table 1	Evaluation and comparison of four advanced LCA methods.	21
Table 2	Absolute Global Temperature Change Potentials AGTP* for 1 kg CO_2 and CH_4 emissions distributed following the delta function, $e(t) = \delta(t)$.	67
Table 3	Absolute Global Temperature Change Potentials AGTP* for 1 kg CO_2 emissions distributed following the negative exponential function, $e(t) = (1/\tau)e^{-t/\tau}$.	68
Table 4	Absolute Global Temperature Change Potentials AGTP* for 1 kg CH_4 emissions distributed following the negative exponential function, $e(t) = (1/\tau)e^{-t/\tau}$.	69
Table 5	Absolute Global Temperature Change Potentials AGTP* for 1 kg CO_2 sequestrations distributed following the Schnute growth function [28], $e(t) = (a/b)e^{-at}(1-e^{-at})^{(1-b)/b}$.	70
Table 6	Specific LCA procedure for mass timber buildings.	71
Table 7	Estimating the average OM of a softwood tree using Alemdag (1983)'s [52] model.	81
Table 8	Estimating the material efficiency of mass timber manufacturing using LCA studies.	84

1 Introduction

In the effort to mitigate climate change, buildings are an important sector to address as they currently contribute to 39% of global greenhouse gas (GHG) emissions [1]. Building-related emissions can be divided into two categories: “operational” and “embodied”. Operational emissions arise from energy use during the building’s useful life, such as for heating, ventilation, and air-conditioning (HVAC) [2]. Building operation accounts for 28% of global emissions [2]. Embodied emissions, meanwhile, refer to those associated with materials and construction processes such as manufacturing, transportation, demolition/deconstruction, and waste processing [1]. These account for the remaining 11% [1]. Efforts to decarbonize the building sector have largely focused on operational emissions, while embodied emissions have been largely overlooked [1] [2]. However, as operational carbon is reduced, embodied carbon will grow in importance as a proportion of total emissions [1]. As found by Röck et al. (2020) [2], the percentage of total life cycle emissions that embodied carbon makes up increases for buildings built to more stringent energy performance standards (see Figure 1 below), sometimes exceeding 90%. To truly achieve an environmentally sustainable building sector, efforts to address embodied emissions must rapidly accelerate [1].

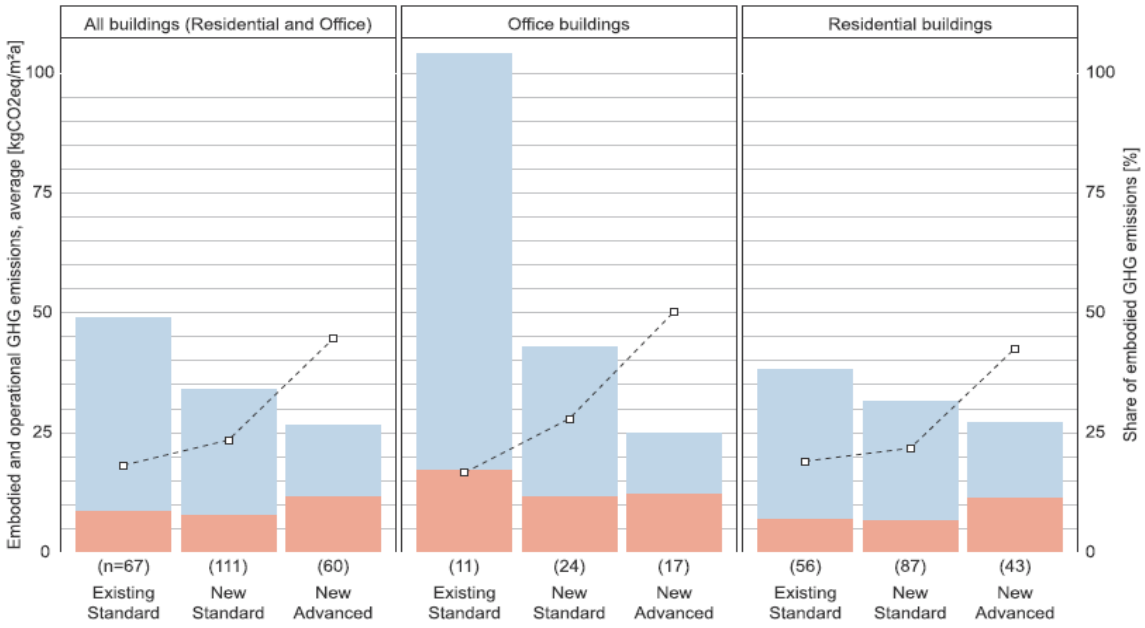

Figure 1: Embodied emissions, both absolute and relative to total life cycle emissions, of buildings built to various performance standards [2].

A key strategy for reducing embodied emissions is using low-carbon construction materials. In recent years, a new category of engineered wood products called “mass timber” has emerged as an alternative structural material to concrete and steel, which are both highly emissions-intensive. Mass timber refers to large-dimensional solid panels and linear elements manufactured by laminating dimensional lumber, veneers, or wood strands. Examples include cross-laminated timber (CLT), glue-laminated timber (glulam), and structural composite lumber (SCL) [3]. Although wood construction was traditionally limited to light-frame, low-rise buildings [4], these products have allowed the structural use of wood to expand into the mid- and high-rise sectors [5]. There are many benefits of mass timber, including the ability to be prefabricated, aesthetic benefits, and biophilic effects on occupants [5]. Most significantly, however, many claim that substituting wood for conventional building materials is highly beneficial from a climate standpoint [3] [6]. These factors have allowed mass timber buildings to proliferate in recent years. The 2020 North American Mass Timber State of the Industry report predicts that globally, the number of new mass timber buildings will double every two years up to 2034 [4]. The Mass Timber Institute at the University of Toronto states that shifting to a low-carbon economy requires buildings to be constructed from wood to the greatest extent possible [5].

Life-cycle assessment (LCA) is a widely accepted method for analyzing the environmental impacts of a building by examining the material and energy flows associated with its life cycle stages. Past LCA studies have shown that mass timber products have much lower manufacturing emissions than concrete and steel. For example, 5 LCA studies on CLT made in North America resulted in global warming potentials (GWP) ranging from 79.99 - 185.69 kilograms of carbon dioxide equivalent ($kgCO_2e$) per cubic meter [7] [8] [9] [10] [11]. In comparison, the Canadian industry average GWP of 40 MPa concrete is 458.98 $kgCO_2e/m^3$ [12], and the North American industry average GWP of hot rolled steel sections is 9516 $kgCO_2e/m^3$ [13]. However, a subject of major contention is the climate impact of biogenic carbon dioxide emissions associated with naturally derived materials. Biogenic carbon dioxide, hereon referred to as $bioCO_2$, is CO_2 that is sequestered from the atmosphere by plants through photosynthesis and subsequently stored in their biomass. Because dry wood consists of approximately 50% carbon by mass [6] [14], the amount of $bioCO_2$ stored in wood products can easily eclipse emissions from other life cycle stages. For example, 1 m^3 of CLT with a dry density of 426 kg/m^3 [9] sequesters 781 kilograms of $bioCO_2$, a quantity much greater than the manufacturing GWPs reported by the previously

mentioned studies. If carbon sequestration is considered a climate benefit, as was done in several studies [6] [10] [15], then wood would appear to be a carbon negative material, and its use would seem to be an effective strategy to mitigate climate change.

Many authors believe that wood products are climate neutral as CO_2 sequestered by tree growth is balanced by that emitted when the products are burned at their end-of-life [16]. Some claim that wood substitution is beneficial because even though the stored bioCO_2 is eventually released, carbon sequestration temporarily avoids some radiative forcing - defined by the Intergovernmental Panel on Climate Change (IPCC) as the change in net downward radiative flux at the top of the atmosphere [17] - and thus causes a cooling effect [18]. Still, others argue that wood use is counterproductive to climate change mitigation. For example, Leturcq (2020) [19] states that the carbon neutrality assumption holds true "only in static conditions, which are seldom met in practice". This author showed using the forest carbon stock evolution after a harvest that the carbon footprint of a wood product is not constant over time (see Figure 2 below). Although it eventually reaches 0, in the short term, it can actually exceed that of a non-wood alternative because bioCO_2 emissions from woody residues created during manufacturing typically occur much sooner than carbon sequestration by forest growth. Furthermore, carbon neutrality would not occur at all if the forest fails to fully regenerate due to changes in climate and tree species, unsustainable forest management, or disturbances [19]. Overall, there is significant debate regarding the true climate implications of using mass timber in place of conventional building materials like concrete and steel.

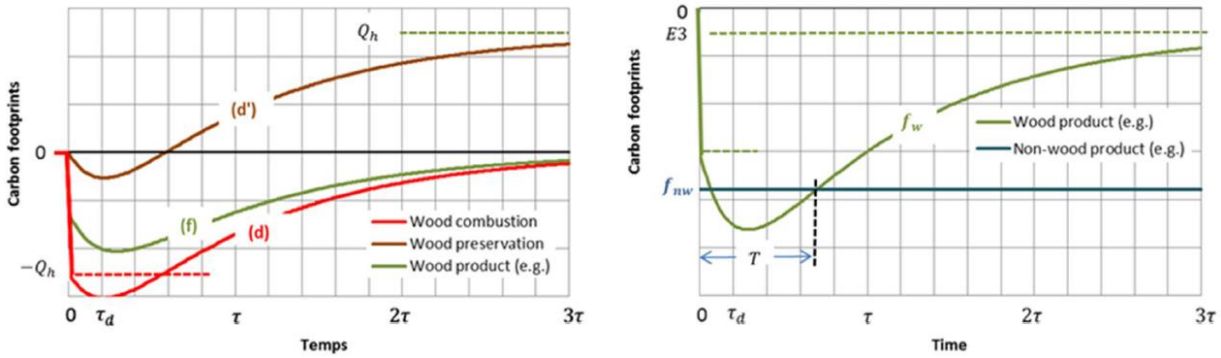

Figure 2: Evolution of the carbon footprint of a wood product over time [19]. The left graph compares the carbon footprint of a wood product (f) to that of wood combustion (d) and an ideal scenario where harvested wood is preserved indefinitely (d'). The right graph compares the

carbon footprint of a wood product (f_w) to that of a non-wood product (f_{nw}), showing that for short time horizons, wood products can be more carbon intensive than non-wood alternatives.

Much of this debate can be attributed to the use of different methodologies to address the impact of timing differences between carbon emission and sequestration. The climate neutrality standpoint results from giving equal weighting to carbon flows regardless of when they occur. Under this practice, as long as the total quantity of bioCO_2 sequestered is equal to that released, the wood product is seen as having a net zero climate impact. The climate-positive standpoint, however, arises from assigning a greater importance to earlier carbon flows - namely, CO_2 sequestration by forest growth, which is assumed to occur prior to building construction - than later ones - namely, bioCO_2 emissions. The climate-negative argument by Leturcq (2020) [19] similarly gives greater weighting to earlier carbon flows. The difference is that in this study, forest growth is assumed to occur following building construction rather than before it.

Unfortunately, the issue of time is not addressed by traditional LCA approaches. In a traditional LCA, an inventory of all GHGs emitted in a building's life cycle is first created. Then, 100-year GWPs are used to convert all emissions into CO_2 equivalents. Finally, these are summed together to produce the global warming result of the building, in kgCO_2e. In this process, all carbon flows are treated equally regardless of their timing [20]. This is valid when climate impacts are being analyzed at time horizons much longer than the typical lifespans of buildings (such as a few hundred or thousand years) since timing differences of a few decades are negligible. However, time-sensitive climate goals, such as the Paris Agreement targets, demand climate impacts to be assessed over timescales comparable to typical building lifespans (for example, 50 to 100 years). Over such short time horizons, a carbon flux occurring early in a building's life cycle will have a much greater cumulative effect on climate variables like surface temperature and sea levels than one occurring decades later at the end of its life. In general, at any finite time horizon, an instantaneous carbon emission does not have the same climate impact as one occurring at a different point in time, or at a small rate over a period of time [21]. The traditional LCA approach of giving equal weighting to time is therefore unreasonable.

Many alternative LCA methods have been proposed to account for the effect of time. These methods are collectively termed 'advanced LCA methods' in this thesis, and several are

reviewed in section 2.2. However, none of them are commonly used in LCA practice, nor are adopted by LCA standards. For example, ISO 21930, which provides core rules for environmental product declarations of construction products and services, states in clause 7.2.9 that the effects of delayed emissions are "not part of the quantification of the GWP", and shall be reported under "Additional environmental information not derived from LCA" [22]. Overall, a lack of consensus regarding the appropriate methodology to account for time in LCA leads to debate regarding the climate implications of wood use in construction. Given the rapidly growing popularity of mass timber, there is a pressing need to ensure that the issue of time in LCA is addressed in a scientific and consistent manner.

The objective of this thesis is to support the creation of a standardized advanced LCA method for assessing the climate impacts of mass timber buildings that uses a science-based approach to account for the effect of time. Such a method should have characteristics that favor adoption by LCA standards, such as low data requirement and computational complexity. Further, as shown in Figure 3 below, the potential to reduce embodied carbon is the greatest at the early stages of a project and diminish over time [1]. While the most effective strategy is to avoid material usage from the outset, it is also important to "build clever" by optimizing material usage and designing with low-carbon materials where possible [1]. Therefore, to support the "build clever" strategy, the advanced LCA method should be appropriate for use by building architects and engineers with limited LCA expertise in the early design stage for comparing the climate impacts of various material choices and design alternatives.

Based on a critical review of LCA methods in section 2, section 3 proposes a new advanced LCA method that accounts for the effect of time. Section 4 presents a sensitivity analysis of a case study mass timber building's climate impact to the time horizon for impact assessment and the rotation period of the forest stand from which the building's materials were sourced, using the proposed LCA method. The primary goal of the sensitivity analysis is to further emphasize the need for advanced LCA methods by illustrating the inability of traditional LCA to represent climate impacts in a realistic manner and to fully capture the variables that influence it. It will also assess the practicality of the proposed LCA method for incorporation into LCA standards and for use by building designers at the early design stage. Further, it will contribute to creating a more objective understanding of the climate implications of the shift to wood construction by

highlighting two key factors that influence global warming impact results for mass timber buildings. Section 6 discusses key insights drawn from the sensitivity analysis, strengths and weaknesses of the proposed LCA method, and areas of future work.

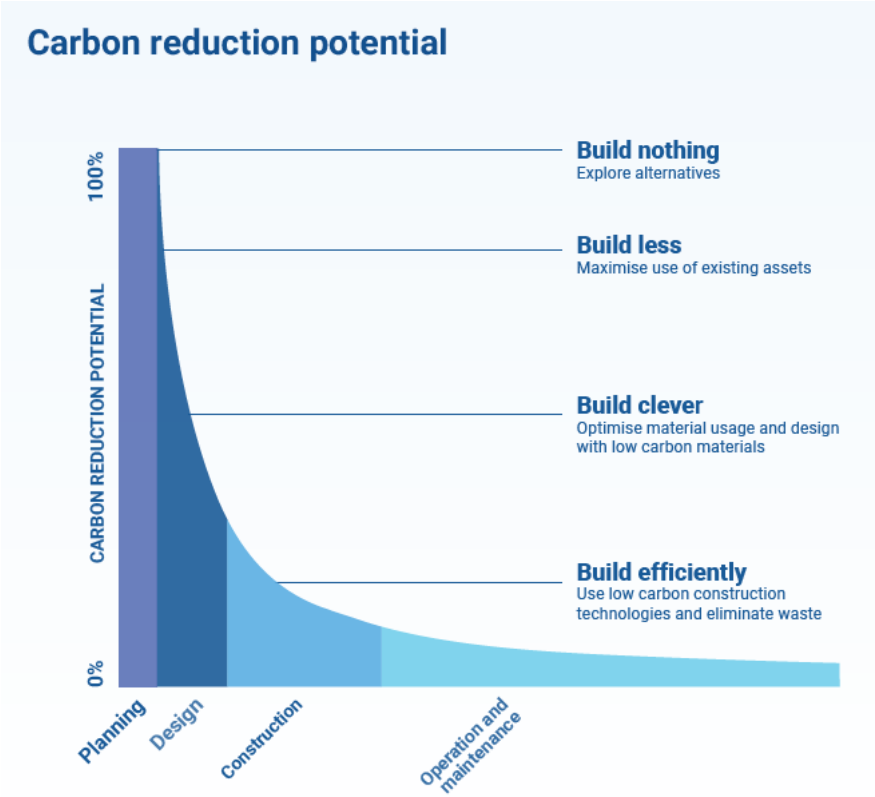

Figure 3: Embodied carbon reduction potential versus phase of a building project [1].

2 Literature Review

2.1 Traditional LCA Methods

Traditional LCA methods encompass two major approaches. The first, called the "0/0" method, excludes bioCO_2 fluxes entirely as it assumes that CO_2 sequestered by tree growth is equivalent to the bioCO_2 that is released at the product's end-of-life [20]. It considers wood to be carbon neutral, and only accounts for emissions from fossil fuels. The second, called the "-1/+1" method, characterizes carbon uptake at the beginning of the product's life as a negative emission, and bioCO_2 release at its end-of-life a positive one [20]. If the absolute quantity of bioCO_2 emitted is equal to that sequestered, this approach likewise treats wood as carbon neutral [20]. The -1/+1 approach has the advantage of being more transparent about bioCO_2 flows [20]. However, it poses a risk of misuse where only carbon sequestration is accounted for but not emissions [20]. This is a common issue in 'cradle-to-gate' LCAs that only include the resource extraction, transportation, and manufacturing stages in their scopes, and neglect the end-of-life stage. In these studies, wood products like CLT may appear to have extremely low or even negative carbon footprints (see for example [10]).

As discussed in section 1, the climate impact of an emission depends on its time of occurrence. Consequently, because bioCO_2 sequestration and emission events occur at different times in the life cycle of a long-lived wood product, they will not result in a net-zero effect on the climate, even if they are equivalent in quantity. The 0/0 approach of ignoring bioCO_2 fluxes altogether is therefore unreasonable. Further, the -1/+1 approach of modelling bioCO_2 flows as a pulse uptake at the beginning of a building's life and a pulse emission at its end is a vast oversimplification. In reality, these flows can be widely distributed over time. For example, forest growth typically occurs over many years, and decomposition of wood waste in landfill will continuously release emissions for decades. Thus, it is also highly unlikely that the -1/+1 approach will accurately produce the climate impact of a mass timber building.

Another issue to point out is that by using a time-*independent* characterization factor, the global warming potential (GWP), traditional LCA does not enable a consistent overall time horizon for impact assessment [21]. In this thesis, the assessment time horizon is defined as the year at which climate impacts are evaluated. For instance, a '2050 time horizon' means that the state of climate

variables like surface temperature or sea levels at this particular year are of interest, and a '28-year time horizon' means that climate impacts are being analyzed 28 years after a building's construction. To elaborate upon the previous point, consider the definition of the GWP as the time-integrated radiative forcing caused by a pulse emission of 1 kg of a GHG over 100 years, also known as its absolute global warming potential (AGWP), divided by the AGWP of 1 kg of CO_2, as shown by equation 1:

$$GWP_x = \frac{AGWP_x}{AGWP_{CO2}} = \frac{\int_0^{100} \alpha_x C_x(t)dt}{\int_0^{100} \alpha_{CO2} C_{CO2}(t)dt} \quad (1)$$

Where:

- x is the GHG that the GWP pertains to,
- α_x and α_{CO2} are the radiative efficiencies of x and CO_2 in [$W/m^2 \cdot kg$], respectively, and
- $C_x(t)$ and $C_{CO2}(t)$ are the impulse response functions (IRF) of x and CO_2, respectively. The IRF models the amount of a GHG, in [kg], remaining in the atmosphere t years after a 1 kg pulse emission. C_{CO2} is given by equation 2 in section 2.2.1 and comes from the Bern carbon cycle (CC) model, which is a well-known model recognized by the United Nations Framework Convention on Climate Change [23].

When the GWP is used to characterize an emission that occurs at year 0, it is implied that the impact of that *emission* - namely, its cumulative radiative forcing - is being analyzed up to year 100. However, applying the same GWP to another emission at year 75 suggests that the impact of this *emission* is being analyzed up to year 175. It is unclear here whether the LCA study is concerned with the climate impact of the *building* at year 100 or 175. If it is the former, then applying the 100-year GWP to the second emission overweighs its importance since its impact should actually be computed over 25 years. If it is the latter, then the 100-year GWP underestimates the importance of the first emission as in this case, its impact should actually be computed over 175 years. This issue is illustrated by Figure 4 below, provided by Levasseur et al. (2010) [21]. Enabling a consistent overall time horizon for the LCA study requires the use of time-dependent characterization factors [21]. In other words, instead of being a fixed 100 years as in the case of the GWP, the integration time interval used to evaluate the characterization factor should depend on the timing of a carbon flux relative to the assessment time horizon.

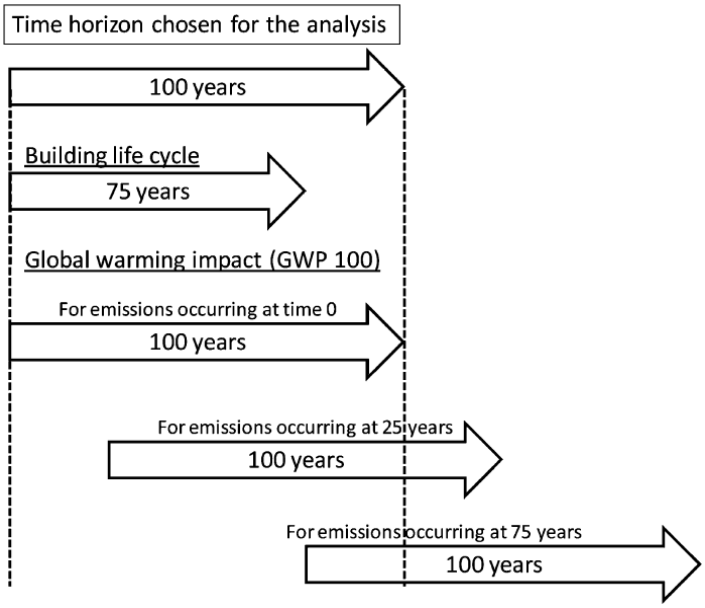

Figure 4: Inconsistency in the overall assessment time horizon of an LCA study due to use of a time-independent characterization factor, the 100-year GWP [21].

In summary, the shortcomings of traditional LCA approaches include firstly its ignorance of the dependence of climate impacts on the timing of a carbon flow, secondly its misrepresentation of the time distribution of the carbon fluxes, and thirdly its lack of a consistent time horizon for impact assessment. These weaknesses make traditional LCA inadequate for accurately assessing the climate impacts of wood products. This in turn limits its ability to objectively compare mass timber and conventional buildings. As evidenced by Leturcq (2020) [19], the climate impact of a building, or any product system, evolves over time and cannot be summed into a single figure. These facts motivate the need for novel LCA methods that do support a consistent time horizon, that more accurately represent the time-distribution of emissions and sequestrations, and that account for the impact of timing differences in a scientific manner.

2.2 Advanced LCA Methods

Several alternative LCA methods have been proposed over the last few decades that attempt to capture the dimension of time. These methods are collectively termed ‘advanced LCA methods’ in this thesis. A study by Andersen et al. (2021) [20] reviewed 226 scenarios of wood building LCAs that used various approaches, both traditional and advanced. It found that while advanced methods produced lower average GWP results per square meter of floor area, methodological

differences caused significant variation among the results [20]. As shown in Figure 5 below, while some advanced methods (referred to by [20] as 'dynamic' methods) produced negative GWPs, some resulted in values similar to those obtained from traditional LCA, while others gave results that are much higher. The existence of significant methodological differences between advanced LCA methods warrant an in-depth literature review and critical comparison between them to determine which one may be the most suitable for inclusion in LCA standards and for use by building designers.

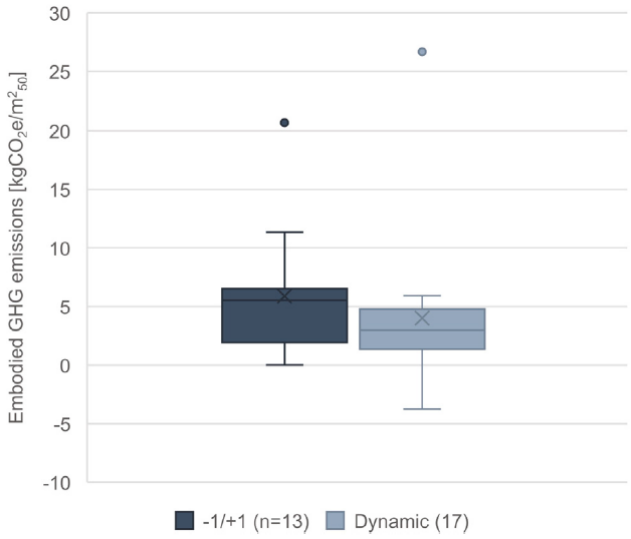

Figure 5: Comparison of GWP results for wood building LCAs using traditional and advanced (dynamic) LCA methods [20].

The following subsections will review 4 advanced LCA methods: the Moura-Costa method by Costa and Wilson (2000) [24], the Lashof method by Fearnside et al. (2000) [25], Dynamic LCA by Levasseur et al. (2010) [21], and the GWP_{bio} method by Cherubini et al. (2011) [26] and Cherubini et al. (2012) [27]. To compare their strengths and weaknesses, each method will be evaluated according to several criteria. To begin, as necessary improvements upon traditional LCA mentioned at the end of section 2.1, an advanced LCA method should:

1. Accurately represent the time-distribution of emission and sequestration events in a building's life cycle - hereon referred to as the building's 'emission profile' - by including both carbon emissions and removals in the analysis and representing their timing in a realistic manner,

2. Support a consistent overall time horizon for climate impact assessment, and
3. Account for the effects of timing differences using well-established scientific theories related to climate change.

Further, to be suitable for incorporation into LCA standards like ISO 21930 [22] and for use by building designers at the early design stage, an advanced LCA method should also:

4. Have low data requirements, meaning that the information it needs is low in volume, requires limited LCA expertise to obtain, and is available at the early design stage, and
5. Have low computational requirements, meaning that it involves few calculation steps and avoids the need for sophisticated software programs.

Criteria 4 and 5 will sometimes be collectively referred to as a method's 'simplicity'.

2.2.1 Moura-Costa Method

The Moura-Costa method developed by Costa and Wilson (2000) [24] accounts for the climate benefits of carbon sequestration and storage by establishing equivalence between tonne-years of CO_2 storage and avoided fossil CO_2 emissions. The key concept behind this method is illustrated by Figure 6 below. In the figure, the curve above the horizontal axis is the impulse response function (IRF) of CO_2, which approximates the atmospheric decay of a 1 tonne pulse CO_2 emission according to the Bern carbon cycle (CC) model [23]. This curve, the equation for which is shown below the figure, is the sum of several exponentially decaying functions that model the responses of various terrestrial carbon sinks to a CO_2 emission, as well as a constant that represents the fraction of the emission that remains indefinitely in the atmosphere [23]. The area under the curve from year 0 to year 100 is approximately 55 tonne-years [24]. Assuming that the radiative efficiency of CO_2 is independent of time, the authors argue that therefore, every 55 tonne-years of CO_2 storage is equivalent to avoiding 1 tonne of fossil CO_2 emissions [24]. Equivalently, every 1 tonne-year of CO_2 storage is the same as avoiding 0.01825 tonnes of fossil CO_2 [24]. The value 0.01825 $year^{-1}$ is called the 'equivalence factor' E_f, and is used to compute negative GWP contributions by carbon storage events.

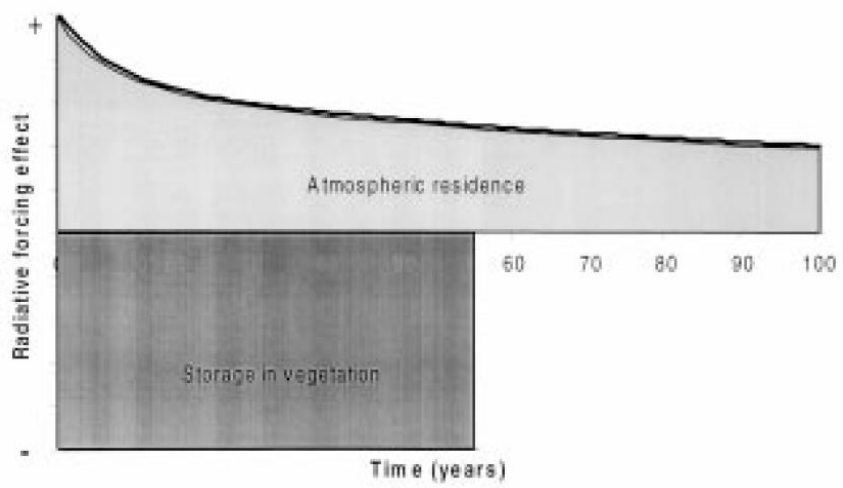

Figure 6: The concept of equivalence between carbon storage and avoided fossil emissions, proposed by [24]. Note that the two grey areas are equal.

$$C_{CO2}(t) = A_0 + \sum_{i=1}^{3} A_i e^{-t/\tau_i} \quad (2)$$

Where:

- A_0 = 0.217 is the fraction of a pulse CO_2 emission that indefinitely remains in the atmosphere, and A_1 = 0.259, A_2 = 0.338, and A_3 = 0.186 are the capacities of various terrestrial carbon sinks [27], and
- τ_1 = 172.9, τ_2 = 18.51, and τ_3 = 1.186 years are the characteristic CO_2 uptake times of the respective carbon sinks [27].

The main advantage of the Moura-Costa method is its simplicity. For a mass timber building, using this method only requires knowledge of the carbon mass that it contains, which can be obtained from a material take-off, and the building's expected lifetime, which can be approximated at the design stage. Applying it only requires multiplying the number of tonne-years of carbon storage by the equivalence factor, making the method easy to use. However, the Moura-Costa method has numerous shortcomings. Firstly, it only accounts for carbon removals and not emissions, meaning that a separate method is needed to complement it. Secondly, it does not enable a consistent assessment time horizon since the equivalence factor is time-independent. In other words, because the equivalence factor is the same regardless of the time at which a carbon removal occurs, the Moura-Costa method would analyze two sequestration events occurring at different times over different time horizons, like the situation depicted in Figure 4.

Another weakness is that in the derivation of the equivalence factor, while the effect of terrestrial carbon sinks in absorbing atmospheric CO_2 following a pulse emission is considered, their response to a sudden CO_2 removal is not. As shown by Figure 6 above, it is assumed by [24] that a sequestration event causes a step change in the atmospheric carbon pool, which remains constant for the duration of storage before returning to its original level via another step change caused by release of stored carbon. Such a pattern is not realistic because as pointed out by Cherubini et al. (2011) [26], a sudden decrease in atmospheric CO_2 concentration leads to carbon being released from the upper ocean layer, which gradually restores atmospheric CO_2 levels. To illustrate the issue, if removing 1 tonne of CO_2 and storing it for 55 years avoids the climate impact of a 1 tonne fossil CO_2 emission over 100 years, then it may be said that conversely, releasing 1 tonne of CO_2 and recovering it 55 years later results in the same climate impact that a 1 tonne fossil CO_2 emission has over 100 years. The logical flaw in this statement highlights the shortfall of the Moura-Costa method in its scientific rigor.

Furthermore, the Moura-Costa method can only be applied if the building does indeed result in additional carbon storage that would not have taken place otherwise. This depends on the baseline forest scenario upon which the assessment is conducted. If the wood used in a building was derived from an afforestation project - in other words, if the forest stand would not have existed without the increase in wood demand caused by the building - then a carbon storage credit can be claimed. However, if raw materials were instead extracted from a pre-existing forest stand that would have stayed intact it were not for the building, then the building should not be given this credit as it did not result in additional carbon storage. In the latter case, the Moura-Costa method would not be applicable. Overall, despite its simplicity, the many limitations of the Moura-Costa method make it unsuitable for LCAs of mass timber buildings.

2.2.2 Lashof Method

The Lashof method proposed by Fearnside et al. (2000) [25] regards the benefit of temporary carbon storage as its ability to delay radiative forcing caused by an emission beyond a certain time horizon. This is illustrated by Figure 7 below. In the example given, when a 100-year time horizon is used and a 1 tonne CO_2 emission at year 0 is delayed by 46 years due to carbon storage, 17 tonne-years' worth of radiative forcing is pushed beyond the time horizon. As per the definition of the time horizon as the year at which climate impacts are evaluated, all radiative

forcing that occur after it are not included in the LCA. Accordingly, the 17 tonne-years of delayed radiative forcing is considered a climate benefit of the carbon storage mechanism.

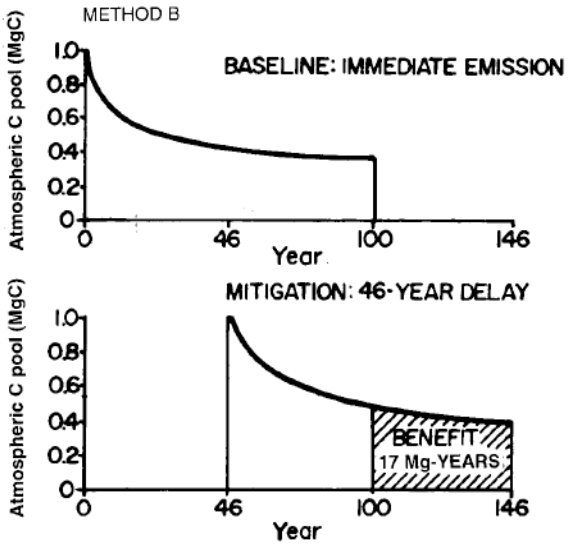

Figure 7: The benefit of carbon storage viewed by [25] as delaying the radiative forcing caused by an emission beyond the assessment time horizon.

The concept behind the Lashof method is relatively simple to understand. Its computational demand is low as the radiative forcing avoided by delaying emissions by various amounts of time can be computed in advance and presented in tabulated format. Applying it would then only require knowledge of the total quantity of CO_2 emitted and the number of years by which the emission is delayed. Its main advantage over the Moura-Costa method is that it supports a consistent time horizon for impact assessment. The practice of discounting climate impacts by simply pushing them beyond the time horizon is not logically flawed as far as the definition of the time horizon is concerned. However, it does indicate a need for the practitioner to exercise care when choosing a time horizon so as to not unintentionally neglect significant climate impacts by simply excluding them from the analysis.

Nonetheless, the Lashof method also has several major shortfalls. To begin, it only considers the climate benefit of delaying pulse CO_2 emissions. Distributed emissions as well as sequestrations, such as those arising from periodic maintenance activities and forest growth, are not addressed. Moreover, the Lashof method requires knowledge of a baseline scenario in which emissions are not delayed, against which the climate benefit of carbon storage is calculated. For a building, it is

unclear what a baseline scenario would be. One possible viewpoint is that using wood in construction delays emissions compared to the case where wood is burned, but using such a baseline is hard to justify as the forest might not have been harvested in the first place if building was not proposed. Fearnside et al. (2000) [25] proposed the Lashof method for assessing the climate benefits of forest conservation projects. For this type of project, the baseline scenario is apparent as it would be the case where the forest is clearcut and the stored CO_2 is released instantly. However, because baseline emission scenarios are typically not available for construction projects, the Lashof method is unsuitable for LCAs of mass timber buildings.

2.2.3 Dynamic LCA

The dynamic LCA method developed by Levasseur et al. (2010) [21] captures the climate impacts of temporally differentiated emissions and supports a consistent time horizon by using 'dynamic characterization factors' (DCF). Unlike the 100-year GWP, the DCF is time-dependent, meaning that its value varies with the time at which an emission occurs. The approach essentially gives a weighting to time where earlier emissions take on greater importance than later ones [21]. The DCF is defined as the cumulative radiative forcing, or absolute global warming potential, associated with a greenhouse gas *i* over *t* years, and is denoted $[DCF_i]_t$ [21]. It is calculated using the following equation:

$$[DCF_i]_t = AGWP_i(t) = \int_0^t a_i C_i(t')dt' \quad (3)$$

Where:

- a_i is the radiative efficiency of *i* in [W/m^2·kg], and
- $C_i(t')$ is the impulse response function of *i*.

The IRF of CO_2 is given by equation 2, which comes from the Bern CC model. For other GHGs like methane (CH_4), $C_i(t)$ is given by a first order decay equation with perturbation lifetime of τ, which is the time at which the quantity of gas remaining in the atmosphere has decayed to 1/e of the original quantity emitted [21], as follows:

$$C_i(t) = e^{-t/\tau} \quad (4)$$

The climate impact result of a building is computed by dividing the assessment time horizon *TH* into 1-year timesteps, determining the amount of each gas emitted at every timestep *j*, multiplying this amount by the DCF of the gas computed using equation 3 with *t = TH - j*, and then summing the results together. This process is depicted by the following equation:

$$GWI(TH) = \sum_i GWI_i(TH) = \sum_i \sum_{j=0}^{TH} [g_i]_j [DCF_i]_{TH-j} \quad (5)$$

Where:

- GWI(TH) is the global warming impact, in units of [(W/m^2)·year], of a product or building at some time horizon *TH*,
- GWI$_i$(TH) is the global warming impact of greenhouse gas *i* at *TH*,
- *j* denotes 1-year timesteps, and
- $[g_i]_j$ is the amount of *i*, in [kg], emitted in year *j*.

The main strength of the Dynamic LCA method is that by discretizing the time horizon into many timesteps, it can represent the emission profile of a building with a very high level of accuracy. Further, it is a very general method that can be applied to emission profiles of any arbitrary shape as long as the amount of each gas emitted at each time step is known [21]. Although formulated for emissions and not removals, sequestration events can also be accounted for by using the 'net emission profile', that is, the amount of carbon emitted at each time step minus the amount sequestered. Due to its generality, the Dynamic LCA is applicable to all projects for which a net emission profile can be determined [21].

The most significant limitation of Dynamic LCA is that it is highly data demanding. Applying the method requires knowledge of the exact amount of every GHG emitted and sequestered at every time step within the time horizon. This information would be extremely difficult to obtain with high accuracy at the design stage. Although it is possible to approximate the net emission profile, doing so would require substantial knowledge of the carbon flows associated with all life cycle stages of a building - such as forest growth patterns and decay mechanisms of wood in landfill – on part of the designer. Therefore, despite its generality, Dynamic LCA is unsuitable for use by building designers to at the early design stage.

2.2.4 GWP_{bio} Method

The GWP_{bio} method created by Cherubini et al. (2011) [26] proposes a characterization factor, the GWP_{bio}, that converts $bioCO_2$ emissions into fossil CO_2 equivalents. This is similar in concept to the commonly used 100-year GWP, which converts non-CO_2 gases like CH_4 into CO_2 equivalents. Like the GWP, the GWP_{bio} is computed by dividing the cumulative radiative forcing caused by $bioCO_2$ emissions by that caused by fossil CO_2.

The carbon flux scenario upon which the GWP_{bio} method was created is one where biomass is harvested from an even-aged vegetation stand and burned to instantly release its stored carbon [26]. The stand is then replanted with the same vegetation species, and eventually captures the same amount of CO_2 that was released [26]. This is shown in the following figure.

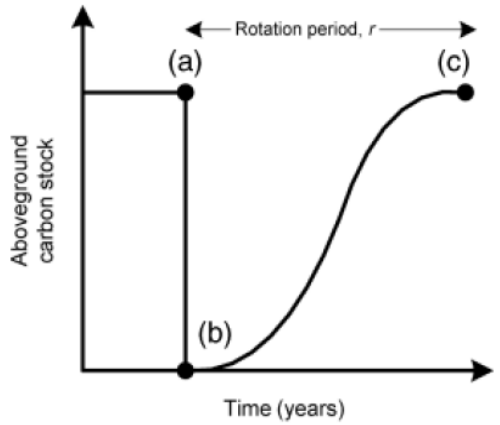

Figure 8: Carbon flux system upon the original GWP_{bio} method was developed by [26].

According to [26], unlike fossil CO_2 which decays according to the Bern CC model (equation 2), the atmospheric decay of $bioCO_2$ is subject to both the effects of terrestrial carbon sink dynamics and CO_2 reabsorption by biomass growth. The IRF of the $bioCO_2$ is thus expressed as the convolution of the net emission profile with the IRF of fossil CO_2:

$$C_{bio}(t) = \int_0^t (C_0\delta(t') - g(t'))C_{CO2}(t - t')dt' \quad (6)$$

Where:

- C_0 is the quantity of the $bioCO_2$ emission in [kg],
- $\delta(t')$ is the delta function, which models the $bioCO_2$ emission as a pulse occurring at t = 0,

- g(t') is the biomass growth function, which models the rate of CO_2 sequestration over time and has units of [kg/year]. In [26], g(t) is assumed to be a Gaussian distribution:

$$g(t) = \frac{1}{\sqrt{2\pi\sigma^2}} e^{-(t-\mu)^2/2\sigma^2}$$

- The term ($C_0\delta(t') - g(t')$) is the net emission profile, and
- C_{CO2} is the IRF of fossil CO_2 emissions, given by equation 2.

The GWP_{bio} is then defined as the ratio of the AGWP of $bioCO_2$, computed by integrating equation 6 with the radiative efficiency of CO_2 over some time horizon *TH*, to the AGWP of fossil CO_2 over the same time horizon [26]:

$$GWP_{bio} = \frac{AGWP_{bio}}{AGWP_{fossil}} = \frac{\int_0^{TH} \alpha_{CO2} C_{bio}(t)dt}{\int_0^{TH} \alpha_{CO2} C_{CO2}(t)dt} \quad (7)$$

This factor is multiplied with the quantity of $bioCO_2$ emitted to determine its fossil CO_2 equivalent [26]. GWP_{bio} factors for various rotation periods and time horizons can be calculated in advance and presented in tabulated format, as was done by [26], to minimize the amount of computation required by the LCA practitioner.

Cherubini et al. (2012) [27] further developed the GWP_{bio} method by creating GWP_{bio} factors for time-distributed $bioCO_2$ emissions in addition to pulse emissions. This was done because pulse emissions do not realistically represent the emission profile of many products like construction materials, and according to [27], it generally overestimates climate impacts. The authors investigated the use of four probability distribution functions (PDFs) to model distributed $bioCO_2$ emissions: the delta function (for pulse emissions), the uniform distribution, the negative exponential distribution, and the chi-squared distribution. These are shown in Figure 9.

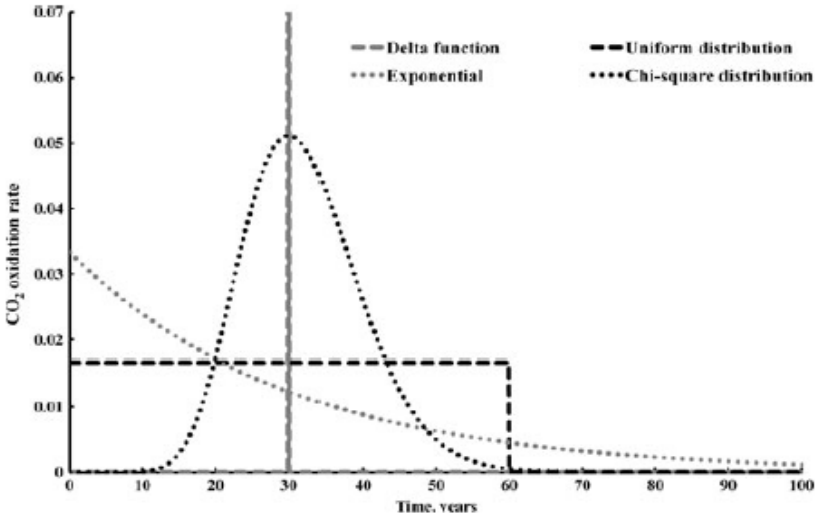

Figure 9: PDFs used to represent distributed bioCO_2 emissions investigated by [27].

Like in the previous study, atmospheric decay functions of bioCO_2 were constructed by convoluting the net emission profile with the IRF of fossil CO_2, as shown by equation 8 below. Equation 8 is essentially the same as equation 6 above, except that δ(t) has been replaced by e(t), which represents the PDF of interest. For distributed emissions, decay functions are referred to as 'perturbation response functions' (PRF) instead of impulse response functions.

$$C_{bio}(t) = \int_0^t (C_0 e(t') - C_0^* g(t')) C_{CO2}(t - t') dt' \quad (8)$$

Where:

- C_0 is the total quantity of bioCO_2 emitted,
- e(t') is the PDF representing the distribution of bioCO_2 emissions,
- C_0* is the total quantity of bioCO_2 sequestered by biomass regrowth,
- g(t') is the biomass growth function. [27] used the growth model developed by Schnute (1981) [28]:

$$g(t) = \delta\beta\gamma e^{\gamma t}(\alpha + \beta e^{\gamma t})^{\delta - 1}$$

- The term (C_0e(t') - C_0*g(t')) is the net emission profile, and
- C_{CO2} is the IRF of fossil CO_2 emissions, given by equation 2.

As in the first study [26], GWP_{bio} factors were created by dividing the AGWP of bioCO_2 by the AGWP of fossil CO_2. These factors are applied in the same manner as those developed in [26]. By multiplication with the total quantity of bioCO_2 emitted, the fossil CO_2 equivalent of a

distributed bioCO_2 emission can found. Again, to reduce computational load, GWP_{bio} factors can be calculated in advance for various PDFs, mean storage lifetimes, and time horizons and presented in tables, as done by [27].

Like Dynamic LCA, the GWP_{bio} method supports a consistent assessment time horizon by employing a time dependent characterization factor. By convoluting the *net* emission profile with the IRF of fossil CO_2, equations 6 and 8 indicate that *both* carbon release and uptake events are subject to the responses of terrestrial carbon sinks. This is an improvement over the Moura-Costa method. The GWP_{bio} factor is similar to the common 100-year GWP, making the method simple to understand and use. Most significantly, however, the GWP_{bio} method overcomes the main limitation of Dynamic LCA of being too data intensive. By approximating the net emission profile using probability distribution functions, the need to evaluate exact quantities of emissions and removals at every timestep is eliminated. Applying the GWP_{bio} method involves first determining which PDF best represents the emission profile of a product or building, selecting a GWP_{bio} factor from tables based on the emission profile and time horizon, and then multiplying the factor by the total quantity of bioCO_2 emitted. As this is a relatively simple process, the method may be highly suitable for use by LCA standards and building designers.

The GWP_{bio} does have several weaknesses, however. Firstly, it only addresses bioCO_2 emissions and not fossil CO_2 emissions. Secondly, as mentioned in both [26] and [27], the GWP_{bio} is based on the assumption of carbon flux-neutrality, which means that biomass regrowth eventually recaptures the same quantity of CO_2 that was emitted. Complete forest regeneration may not always occur, however, due to many possible factors such as changes in climate and tree species, unsustainable management practices, land-use change, and disturbances [19]. Thus, using GWP_{bio} requires a means of guaranteeing that the forest stand will regenerate within the expected harvest interval.

Furthermore, a PDF can only be, at best, a rough approximation of the actual emission profile of a building. As indicated by [27], results obtained using GWP_{bio} are strongly influenced by the selected PDF, especially when the lifetimes of wood products are long. Thus, substantial error would result if the selected PDF poorly models a building's emission profile. The authors [27] recommend the chi-squared distribution (see Figure 9) for modelling the oxidation rate of wood

products. However, it is unlikely that this function will precisely represent the actual emission profile of a mass timber building. For instance, suppose that a large quantity of CO_2 is released during the production stage of a building, a low but steady emission occurs during the building's use stage, and another pulse of CO_2 is released when its wooden components are burned at its end-of-life. In this case, the emission profile would exhibit two peaks with a valley in between, which would look very different from the chi-squared distribution. It may be possible to develop GWP_{bio} factors for a wider range of PDFs, but this would result in a large number of GWP_{bio} tables and make the method tedious to use. A solution to more accurately approximate the emission profile of a building is therefore needed. Table 1 below summarizes the strengths and weaknesses of the 4 advanced LCA methods reviewed in this section.

Table 1: Evaluation and comparison of four advanced LCA methods.

Criterion	**Method**			
	Moura-Costa	**Lashof**	**Dynamic LCA**	**GWP_{bio}**
1. Accurately represents the emission profile (1 to 5)	1 - only accounts for CO_2 removals, not emissions	1 - does not include distributed emissions or sequestrations	5 - highly accurate due to small timesteps; applies to any emission profile	3 - PDF may not be representative of emission profiles
2. Uses a consistent time horizon (Y/N)	N	Y	Y	Y
3. Is scientifically rigorous (1 to 5)	2 - ignores carbon sink dynamics for carbon removals	5	5	5
4. Has low data requirements (1 to 5, 1 = low)	1 - only requires quantity of CO_2 stored and time of storage	5 - requires a well-defined baseline scenario	5 - requires emissions and removals at each timestep	1 - only requires total quantity of bioCO_2 emitted
5. Has low computational requirements (1 to 5, 1 = low)	1 - simply multiply tonne-years of storage by the equivalence factor	2 - integration is needed to get benefit of delayed emissions, but can be done in advance	3 - integration is needed to get DCFs, but can be done in advance. Also, many timesteps means many calculations	1 - simply multiply the quantity of bioCO_2 by the GWP_{bio} factor

2.3 Summary of Literature Review

Traditional LCA has numerous shortcomings that limit its ability to accurately assess the climate impacts of wood product systems. It ignores the time-dependence of climate impacts, represents emission profiles in an oversimplified manner, and lacks a consistent time horizon for impact assessment. The need to more objectively compare the climate impacts of mass timber and traditional materials necessitates the development of advanced LCA methods that account for the effect of time. Although many such methods have been proposed, significant methodological differences exist, and none of them are currently widely used in the industry.

This literature review critically evaluated 4 advanced LCA methods using five criteria. While the Moura-Costa method is simple to use and understand, it only accounts for carbon removals and not emissions, does not support a consistent time horizon, has scientific shortfalls, and is only applicable when a carbon sequestration credit can be claimed. The Lashof method is similarly simple to use and does enable a consistent time horizon, but only deals with pulse emissions and requires a baseline scenario against which the climate benefits of delaying emissions are computed. These critical flaws make both the Moura-Costa and Lashof methods unsuitable for LCA studies of mass timber buildings.

The Dynamic LCA method supports a consistent time horizon by using a dynamic characterization factor whose value depends on an emission's time of occurrence. It can be used with any net emission profile and can represent emission profiles with high accuracy. However, its requirement for emissions to be quantified for many timesteps limits its practicality. The GWP_{bio} method presents a characterization factor for $bioCO_2$ emissions that is very similar to the 100-year GWP. It enables a consistent time horizon and is simple to use. Most significantly, it overcomes the high data requirement of Dynamic LCA by using PDFs to approximate emission profiles. As GWP_{bio} factors can be computed and tabulated in advance, this method also has low computational demand. Despite having several weaknesses, the simplicity of the GWP_{bio} makes it the most suitable method for incorporation into LCA standards and for use by building designers. The GWP_{bio} method thus serves as inspiration for the new LCA method proposed in this thesis. Section 3 discusses the proposed LCA method, highlighting how it addresses some of the limitations of the GWP_{bio}.

3 Proposed LCA Method

The LCA method proposed in this section retains the most advantageous aspect of the GWP_{bio} method, its use of PDFs to model the emission profiles of buildings and products. Like the GWP_{bio}, the proposed method uses distribution functions and tabulated characterization factors to achieve low computational load. However, to improve upon the GWP_{bio}, the proposed method differs from it in four ways. These differences are explained in the following subsections. The strengths and weaknesses of the proposed method are evaluated in section 6.2.

3.1 Differences from the GWP_{bio} Method

3.1.1 Use of Multiple 'Emission Functions'

As mentioned, a source of error associated with the GWP_{bio} method is that a single PDF is unlikely to model the emission profile of a mass timber building with high accuracy. To address this issue, the proposed method approximates the emission profile using multiple distribution functions, hereon referred to as 'emission functions'. Each emission function models the time-distribution of emission arising from one GHG-producing or sequestering process, referred to as an 'emission event'. For instance, a delta function may represent CO_2 released through combustion when wooden components are burned, and a negative exponential function may represent emissions from decay processes, such as when forest residues like branches and foliage decay on the forest floor after a harvest. The superposition of the emission functions associated with all emission events in the building's life cycle forms its emission profile. In other words, the proposed method decomposes the complex emission profile of a building, for which it is difficult to accurately compute climate impacts, into a series of simpler emission functions for which climate impacts can be evaluated to a high degree of accuracy.

The concept of decomposition is illustrated in Figure 10 below. The topmost red curve represents the complex emission profile of a mass timber building, while the three blue curves below it are the emission functions that it can be decomposed into. A closed-form solution for the climate impact of the emission profile is difficult to compute. However, the impacts associated with each of the much simpler emission functions can be easily determined. These impacts can be calculated individually and then summed to produce the total climate impact of the building.

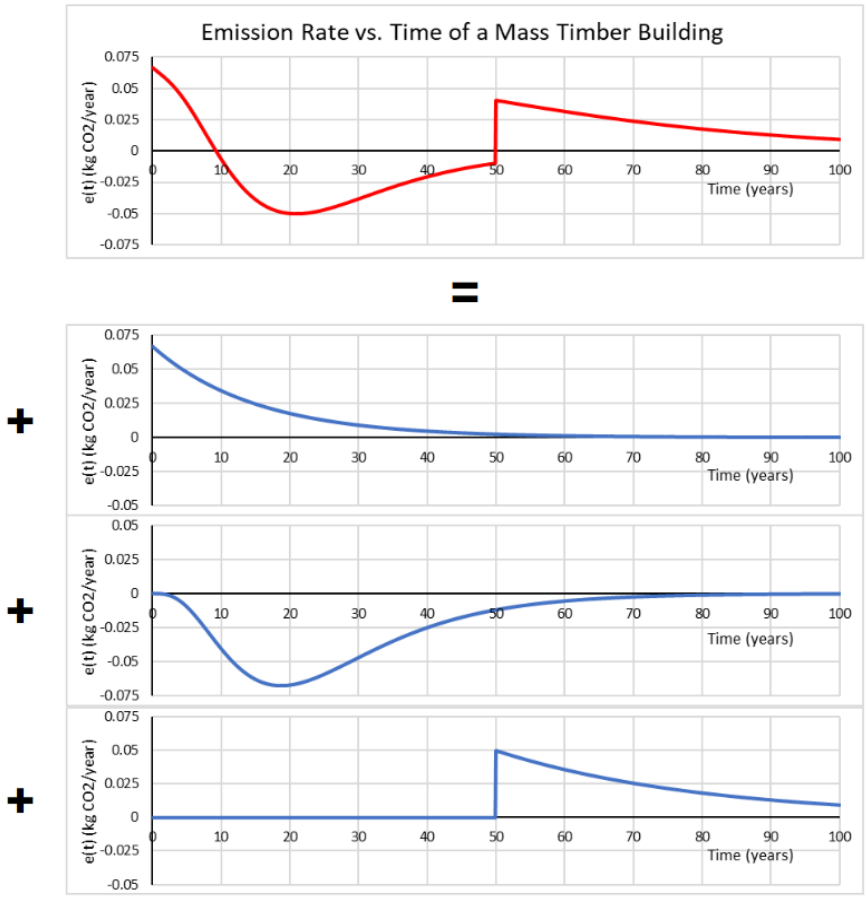

Figure 10: Decomposing a complex emission profile into simple emission functions.

Although using many emission functions instead of a single PDF increases the number of calculations required, the computational load would still be substantially less than that of Dynamic LCA. Doing so, however, enables emission profiles to be modeled with high precision, which would improve the accuracy of results compared to the GWP_{bio} method. The derivation of characterization factors for various emission functions is discussed in section 3.2.

3.1.2 Decoupling of Emissions from Forest Growth

The original GWP_{bio} method computes the PRF using the *net emission profile*, which at any time *t* expresses the rate of carbon emission minus the rate of sequestration (see equations 6 and 8). Because of this, the GWP_{bio} factor simultaneously captures both the climate impact of a bioCO_2 emission and the climate benefit of the corresponding CO_2 uptake. This approach presents two problems. Firstly, as previously mentioned, fossil CO_2 emissions cannot be accounted for as they are not associated with carbon uptake. Secondly, it means that GWP_{bio} factors are only valid

when an emission initiates *at the same time* as carbon sequestration. For example, consider a mass timber building with a lifetime of 50 years, whose wooden components decay aerobically at their end-of-life and release CO_2 following a negative exponential curve (dark blue line in Figure 11), and whose climate impacts at year 100 are of interest. Cherubini et al. (2012) [27] developed GWP_{bio} factors for the negative exponential PDF. However, in doing so, it was assumed that emissions initiate in year 0 (light blue curve in Figure 11), the year in which forest regrowth begins (green curve), while they actually initiate in year 50. As a result, the actual net emission profile of the building (dark red curve) differs from the one assumed by GWP_{bio} (light red curve), meaning that the provided GWP_{bio} factors are not applicable.

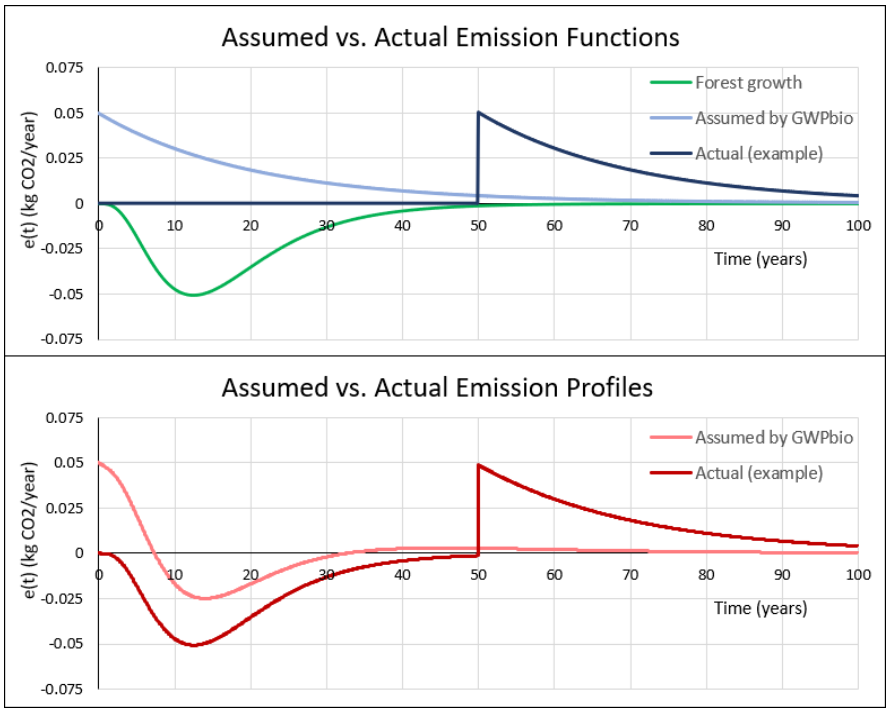

Figure 11: Deviation of an emission profile from the one assumed by GWP_{bio} due to delayed emissions relative to carbon sequestration by forest growth.

While it is possible to incorporate "delay time" as another variable when tabulating characterization factors, doing so would result in a large number of GWP_{bio} tables. Instead, a simpler approach is to separately develop characterization factors for emission and sequestration events. Doing so involves splitting the integral in equation 8 into its two constituents:

$$C_{bio}(t) = \int_0^t C_0 e(t') C_{fossil}(t - t') dt' - \int_0^t C_0^* g(t') C_{fossil}(t - t') dt' = C_e(t) + C_s(t) \qquad (9)$$

Where $C_e(t)$ is the PRF of a bioCO_2 emission, and $C_s(t)$ is the PRF of the corresponding CO_2 sequestration. Characterization factors for emission and sequestration can then be computed separately using their respective PRFs and reported in different tables. In this case, to analyze the example previously mentioned, the LCA practitioner would first select a characterization factor for forest growth for a 100-year time horizon and multiply it by the total mass of CO_2 absorbed. Then, they would select a characterization factor for emissions following the negative exponential function for a 50-year time horizon (since year 100 is only 50 years from the start of the emission at year 50) and multiply it by the total mass of bioCO_2 emitted. Adding these results would then give the total climate impact of the building.

Overall, having separate characterization factors for emission and sequestration events enables analysis of bioCO_2 emissions that do not begin at the same time as carbon uptake. It also allows LCA practitioners to distinguish and better understand the effect of forest growth on the climate impact of a mass timber building. Furthermore, doing so allows fossil CO_2 emissions to be included in the method because when the benefits of carbon uptake is disassociated from the impact of emissions, biogenic and fossil emissions become indistinguishable from a climate standpoint. This aligns with a popular sentiment among LCA literature that the atmosphere treats all emissions the same regardless of whether they originate from fossil fuels or biomass.

3.1.3 Absolute Global Temperature Change Potential

The absolute global temperature change potential (AGTP) gives the change in global surface temperature, in degrees kelvin, due to an emission or sequestration event at some time horizon [27]. It is chosen over the GWP or AGWP as the climate impact metric used by the proposed method for three reasons. Firstly, the GWP_{bio} expresses the AGWP of a bioCO_2 emission over a certain time horizon in proportion to that of a pulse fossil CO_2 emission *over the same horizon*. A problem with this is that GWP_{bio} factors for different time horizons would have inconsistent denominators, meaning that LCA studies that use different time horizons cannot be compared. To elaborate, consider a bioCO_2 emission that is equivalent to 1 kg of fossil CO_2 over a time horizon of 100 years, and another emission that is also equivalent to 1 kg of fossil CO_2 but over a time horizon of 50 years. These two emissions, while both depicted as having a GWP of 1 $kgCO_2e$, are not actually equal in their *absolute* GWPs. This is because the former's is equal to the AGWP of 1 kg of fossil CO_2 over 100 years, while the latter's equal to the AGWP of 1 kg of

fossil CO_2 over 50 years. Consequently, using the GWP_{bio} method, two buildings with the same fossil CO_2 equivalence would not have the same *absolute* climate impact if the assessments were made using different time horizons. The AGTP, on the other hand, overcomes this issue by being an absolute metric, meaning that it does not relate climate impacts to those of fossil CO_2.

Secondly, although the AGWP is also an absolute metric, it is not a tangible measure of the environmental consequences caused by a carbon emission or removal [27]. It is not immediately clear how time-integrated radiative forcing, in units of [(W/m^2)·year], is related to physical changes in climatic variables like surface temperature or sea levels, or social and economic impacts [29]. For this reason, some authors like Peters et al. (2011) [29] question whether the AGWP is an adequate metric for evaluating the efficacy of climate policy. Comparatively, the AGTP is one step further down in the 'cause and effect chain' of a GHG emission [27], shown in Figure 12 below. The AGTP is therefore a more relevant impact metric than the AGWP [27] and has less ambiguity in its interpretation [30].

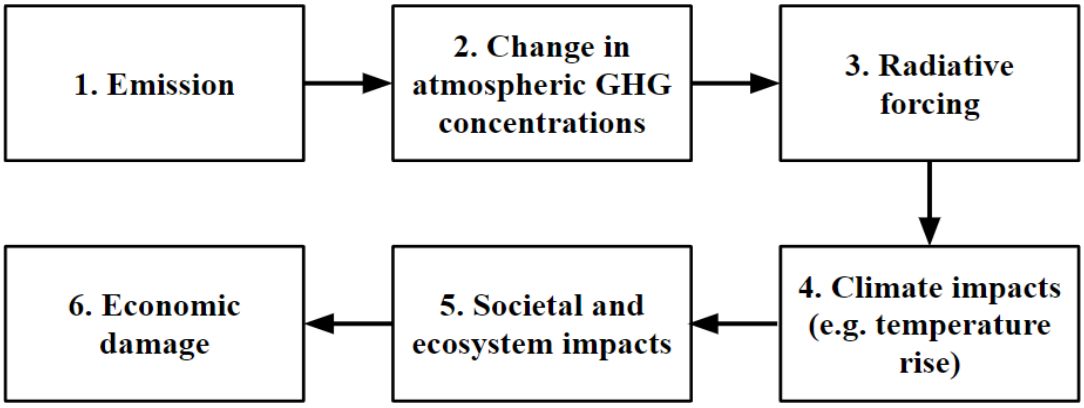

Figure 12: 'Cause and effect chain' of the impacts arising from a GHG emission [30].

Thirdly, when computing the AGWP (see equation 3), radiative forcing is integrated using a constant weighting factor. In other words, all radiative forcing is weighted equally regardless of their time occurrence [30]. However, as with emissions themselves, timing does influence the climate impact of radiative forcing. This is because radiative forcing that occurs earlier gives the climate system more time to relax back to equilibrium [31]. In other words, a 'unit' of radiative forcing occurring at year 0 has a smaller effect on surface temperature at year 100 than the same unit occurring at year 50. By giving equal weighting to time, the AGWP overweighs radiative forcing that occurs early. As a result, two GHGs - one short-lived but stronger, the other long-

lived but weaker - that have the same AGWP will not cause the same surface temperature change at any time horizon [30]. The AGTP, however, places less emphasis on near-term radiative forcing, as shown by the exponential nature of equation 11 below [32]. Overall, the AGTP is chosen as the climate impact metric for the proposed LCA method as it is an absolute metric, is more relevant than the AGWP, and accounts for the timing of radiative forcing.

3.2 Derivation of Characterization Factors

Similar to the definition of the PRF (equation 8), the AGTP of an emission event at some time horizon TH is the convolution of its radiative forcing vs. time function, called its 'radiative forcing profile', with the IRF of surface temperature to radiative forcing [27]:

$$AGTP_i = \int_0^{TH} RF_i(t) \cdot \delta T(TH - t)dt \tag{10}$$

Where:

- *i* denotes the emission event,
- $RF_i(t)$ is the radiative forcing profile of the emission event, equal to its PRF multiplied by the radiative efficiency of the gas emitted:

  $$RF(t) = \alpha_i \cdot C_i(t)$$, and
- $\delta T(t)$ is the IRF of surface temperature to radiative forcing, which was derived by Boucher and Reddy (2008) [31]:

  $$\delta T(t) = \sum_{i=1}^{2} \frac{c_i}{d_i} e^{-t/d_i} \tag{11}$$

  Where $c_1 = 0.631$, $c_2 = 0.429$, in K/(W/m^2), and $d_1 = 8.4$, $d_2 = 409.5$, in years.

According to the IPCC's 6th Assessment Report [17], the radiative efficiencies of carbon dioxide and methane, expressed on a mass basis, are $\alpha_{CO2} = 1.739 \times 10^{-15}$ W/(m^2·kg) and $\alpha_{CH4} = 1.323 \times 10^{-13}$ W/(m^2·kg), respectively. Similar to equation 8, the PRF of an emission event is given by the convolution of its emission function and the IRF of the gas emitted:

$$C_i(t) = \int_0^t e_i(t') \cdot C_{p,i}(t - t')dt' \tag{12}$$

Where:

- $e_i(t)$ is the emission function, which expresses emission rate in units of [kg/year] as a function of time, and
- $C_{p,i}(t)$ is the IRF of the gas emitted. As mentioned, the IRF of CO_2 comes from the Bern CC model and is given by equation 2, while the IRFs of other GHGs like methane are first-order decay functions (equation 4) with time constant τ representing the perturbation lifetime of the gas. As given by the IPCC's 6th Assessment Report, the perturbation lifetime of methane is 11.8 years [17].

Equation 10 is evaluated numerically by discretizing the time horizon into a large number of timesteps. In this paper, AGTP factors are computed for CO_2 and CH_4 as these are the two principal GHGs of interest to the sensitivity analysis. As well, the following three emission functions are considered:

1. The delta function:

$$e_i(t) = \delta(t) \tag{13}$$

2. The negative exponential function:

$$e_i(t) = \frac{1}{\tau} e^{-t/\tau} \tag{14}$$

3. The Schnute growth function presented by Schnute (1981) [28]:

$$e_i(t) = -\frac{a}{b} e^{-at}(1 - e^{-at})^{(1-b)/b} \tag{15}$$

The delta or 'pulse' function models emissions that occur over short periods of time, such as fossil CO_2 emissions incurred during manufacturing and bioCO_2 emissions released when wood is incinerated. The negative exponential function models emissions from decay processes, such as CH_4 released through anaerobic decomposition of wood in landfill [33] and CO_2 emitted by aerobic decay of forest harvest residues [34]. The Schnute growth function developed by Schnute (1981) [28] is used to model the rate of CO_2 uptake by forest growth. The parameters *a* and *b* in equation 15 are calibrated so that the function takes on an 'S'-shape, intersects the horizontal axis at t = 0, exhibits an inflection point at ¼ of the forest rotation period - the time interval before consecutive harvests - and reaches 99% of its asymptotic value at the forest rotation period. Due to a lack of forest growth data, these decisions were made arbitrarily. More precise

calibration of this growth function using empirical studies is recommended for future research. The three emission functions are shown below.

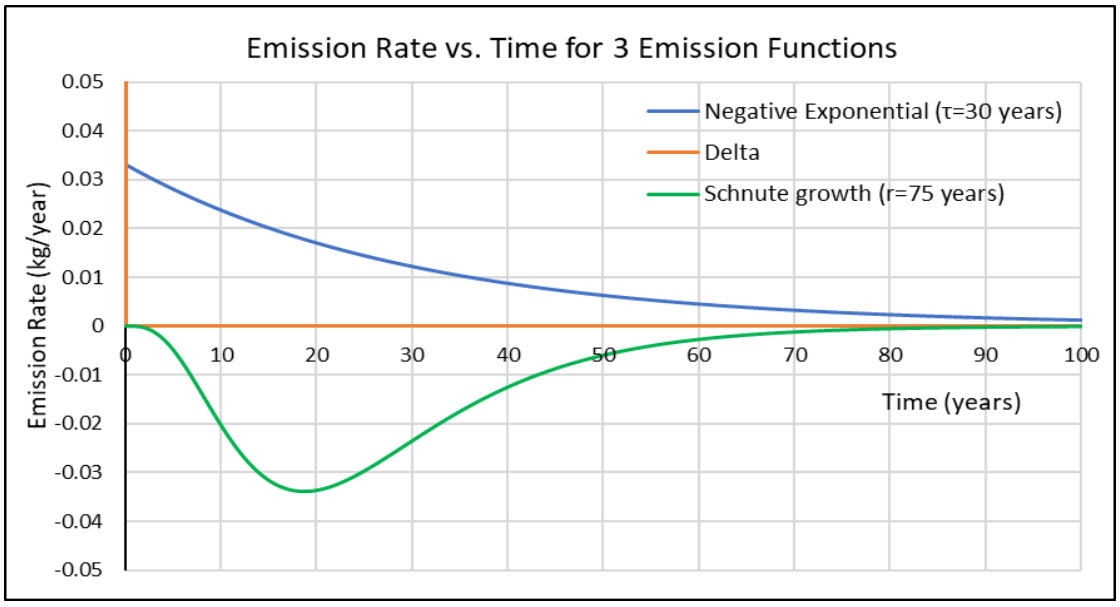

Figure 13: The three emission functions investigated in the present study.

Tables 2 to 4 in Appendix A provide AGTP factors calculated using equation 10 for 1 kg CO_2 and CH_4 emissions distributed following the delta and negative exponential functions. Table 5 provides AGTP factors for 1 kg CO_2 sequestrations distributed according to the Schnute growth function (equation 15). Time horizons up to 200 years are included. Note that the factors for CO_2 sequestration are negative since reduction in atmospheric CO_2 concentration decreases radiative forcing, which in turn causes a cooling effect. These AGTP factors are used in a similar manner to the GWP_{bio} factors presented by [26] and [27]. By multiplying the total quantity of gas emitted or removed in an emission event by an appropriate AGTP factor, the surface temperature change caused by the emission event at some time horizon can be found. Although AGTP factors are only tabulated for CO_2 and CH_4 a limited set emissions function, and only for time horizons up to 200 years, additional tables for other gases and emission functions or for longer time horizons can be developed as necessary.

3.3 General Procedure

The proposed LCA method follows the 6-step process shown in Figure 14 below. This is a general procedure that applies to all types of product systems, including conventional buildings that do not involve bioCO_2 emissions as well as non-building products and services. A variation of the proposed method created specifically for mass timber buildings is detailed in Appendix B.

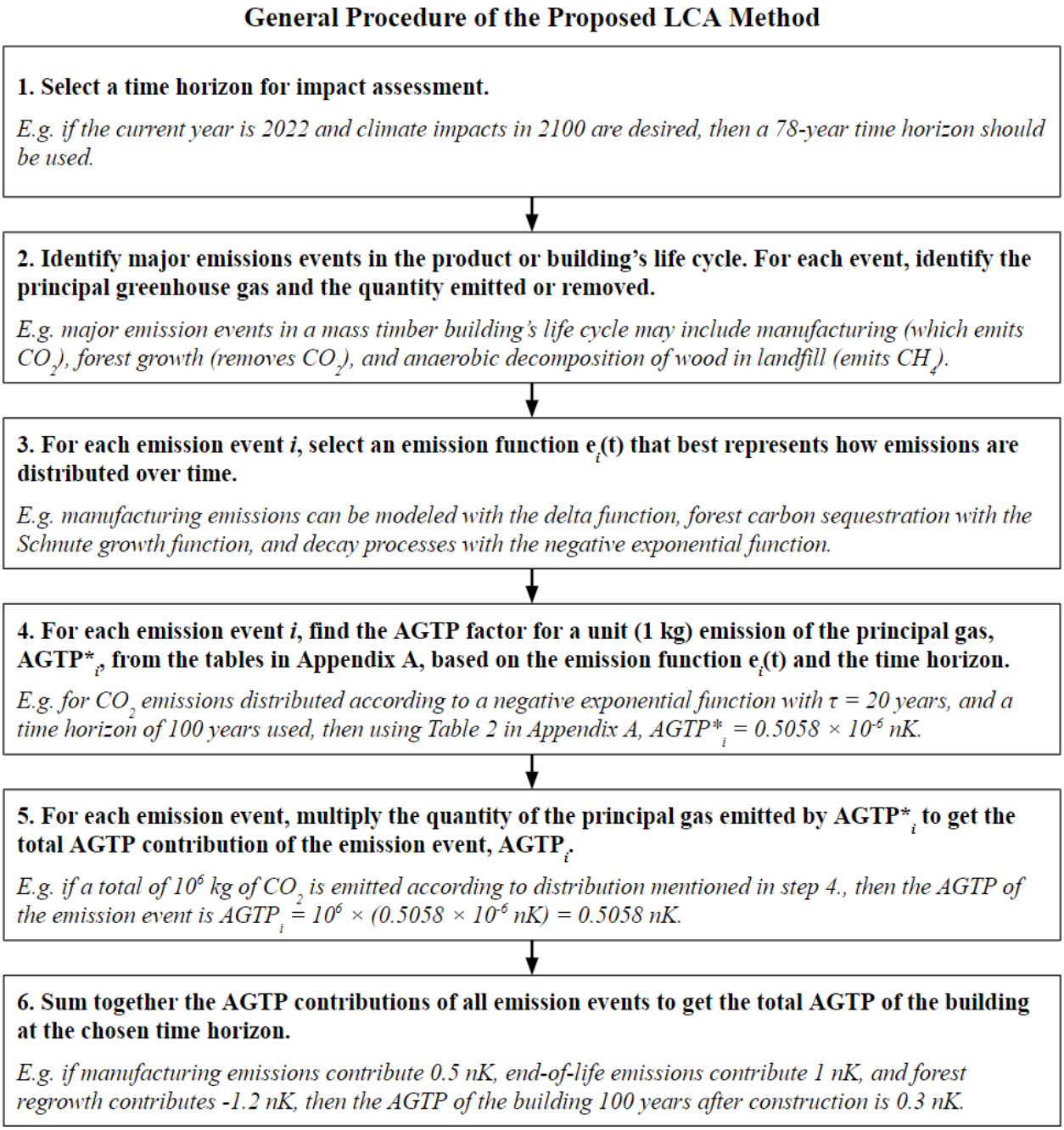

Figure 14: General procedure of the proposed LCA method.

4 Sensitivity Analysis Using the Proposed LCA Method

4.1 Objectives of the Analysis

This section presents an investigation of the sensitivity of the surface temperature impact of a mass timber building to two variables: 1) the time horizon used for impact assessment, and 2) the rotation period of the forest stand from which the wood used in the building was sourced, using the proposed LCA method. These two variables were selected because their influences can only be captured by an advanced LCA method that accounts for the effect of time. For instance, since traditional LCA is only concerned with the total amount of CO_2 sequestered by the forest, it does not acknowledge that the rate of sequestration, indicated by the forest rotation period, also influences climate outcomes. Similarly, as traditional LCA does not account for the fact that the impact of an emission evolves over time, it implicitly assumes that a building's climate impact is the same at all time horizons. The case study building was studied using traditional LCA methods by Chen et al. (2020) [35], and is described in section 4.2. The main objectives of the sensitivity analysis are:

1. To highlight the need for advanced LCA methods by showing the inability of traditional LCA to capture the sensitivity of the climate impact of a mass timber building to the two variables of interest, and
2. To examine the practicality of the proposed LCA method for inclusion in LCA standards and for supporting decision-making at the early design stage, and identify further areas of work needed for it to become more widely adopted.

The first objective will be achieved by first analyzing results obtained using the proposed method in isolation, and then comparing results to that of the original study. The second objective will be achieved by qualitative analysis. In addition, as mentioned, a key motivating issue for this thesis is uncertainty regarding the climate implications of constructing mass timber buildings in place of conventional ones. Addressing this uncertainty requires understanding the various factors that affect the climate outcomes of construction wood products, and their degrees of influence. Thus, in addition to the two stated objectives, this sensitivity analysis aims to build a foundation for such an understanding by analyzing the significance of two key factors: the assessment time horizon and the forest rotation period. Although there are numerous other variables that also

affect the climate impact of mass timber buildings, such as waste treatment scenario [36] and manufacturing methods, they are excluded from this study to enable greater depth of analysis. It is hoped that these factors will be addressed by future research to create a more complete picture of the climate impacts of mass timber buildings.

The following subsections begin by describing the case study building and discussing the LCA scope selected. Section 4.4 explains the rationales for studying the two chosen variables and the values used. Section 4.5 discusses the control variables that are kept constant across all analysis scenarios. The AGTP of one of the scenarios is calculated using the specific method for mass timber buildings (detailed in Appendix B) in Appendix C.

4.2 Description of the Case Study Building

The building analyzed in this investigation, shown in Figure 15 below, is a 12-story mixed-use tower approved for construction in Portland, Oregon, USA [35]. Its structural system consists of CLT panels for floors and walls, and glulam beams and columns [35]. Despite using mass timber above ground, its foundation is made of reinforced concrete [35].

Figure 15: Structural model of the case study building [35].

4.3 LCA Scope

The scope of the original LCA study by Chen et al. (2020) [35] is 'cradle-to-grave', meaning that it includes emissions from the production stage (modules A1-A3 in European LCA standard BS EN 15978:2011, Sustainability of construction works [37]), the construction stage (A4-A5), the use stage (B2, B4, and B6) and the end-of-life stage (C1-C4). To enable comparison the LCA scope used in this study is also 'cradle-to-grave'. However, the use stage (B2, B4, and B6) and the end-of-life stage (C1-C4), aside from bioCO_2 emissions from treatment of used mass timber components, are excluded from the LCA scope. Emissions from stages B2 - Maintenance and B4 - Replacement are ignored because at the early design stage, it is nearly impossible to predict the exact repair and maintenance activities that will occur throughout the building's life. Likewise, B6 - Operational energy use is largely determined by practices of the building operator rather than by the materials used in the building's structure. Similarly, as mass timber buildings are relatively new, it is too early to know exactly how much CO_2 will be emitted by processes used to deconstruct them and transport their parts to waste processing facilities.

Chen et al. (2020) found that both use stage (B2 and B4) and end-of-life (C1-C4) emissions were similar between mass timber and reinforced buildings, and that these emissions are significantly smaller than those from other stages like the production stage (A1-A3) [35]. Use stage and end-of-life stage emissions are therefore excluded as they do not provide meaningful comparison between mass timber and conventional buildings. Thus, the case study building's AGTP is assumed to be only comprised of contributions by:

1. Manufacturing, transport, and construction (MTC) (A1-A5) emissions, including those associated with both mass timber and non-wood components (e.g. concrete foundation, windows, cladding, etc.).
2. BioCO_2 emissions from treatment of woody residues, including those from forest harvest, lumber production in sawmills, and manufacturing of mass timber components,
3. CO_2 uptake by forest regrowth after harvest, and
4. BioCO_2 emissions from treatment of end-of-life mass timber building components.

To match the present study's scope, B2, B4, and C1-C4 emissions were subtracted from the original study's 'A to D' result, producing a GWP value of 4.767×10^5 kgCO_2e.

4.4 Variables of Interest

4.4.1 Assessment Time Horizon

As defined in section 2.1, the assessment time horizon is the year at which climate impacts are analyzed. Because the climate impact of an emission changes over time, the time horizon chosen can significantly influence the results of an advanced LCA study. The selection of a time horizon should be based on a balance between capturing the complete climate impacts of a building and ensuring that the results are relevant to short-term climate policies. A very long time horizon, for example 1000 years, would completely capture the climate impacts of most buildings. However, climate impacts 1000 years from now are meaningless when climate policies are concerned with the consequences of climate change in 50 to 100 years. Selecting a short time horizon, for example 50 years, ensures that the LCA's results are highly relevant. However, doing so risks neglecting significant climate impacts from a building's end-of-life stage. To inform the selection of appropriate time horizons for LCAs of mass timber buildings, this study will analyze how using various time horizons influence the LCA results of the case study building.

The IPCC frequently uses 2100 as the year for assessing the effect of climate change on environmental variables like surface temperature and sea level rise. For example, in its 2018 Special Report on the impact of global warming of 1.5^{o}C, 2100 was used as the timeline for modelling global temperature trajectories under various anthropogenic GHG emission scenarios [38]. Following the IPCC's convention, the present study chooses 2100 - 78 years from the present year, 2022 - as one of time horizons. Three other values are also selected: 28 years (representing year 2050 relative to 2022), 128 years (2150), and 178 years (2200). 28 years is chosen to illustrate the consequence of neglecting the end-of-life stage by using a time horizon shorter than the building's lifespan (discussed in section 4.5.1), while 128 and 178 years are used to assess the benefit of using longer time horizons to more completely capture the building's climate impacts.

4.4.2 Forest Rotation Period

Forest rotation period is the time interval between successive harvests of a forest stand and indicates the speed of carbon uptake. It influences the climate impact of a mass timber building because under a finite time horizon, carbon removals occurring earlier will exert greater

cumulative radiative forcing than those occurring later. However, as mentioned in section 3.1.3, when global surface temperature change is of interest, earlier radiative forcing has lower impact since it gives more time for the climate system to relax [31]. The effect of forest rotation period on the AGTP of a mass timber building is thus unclear and is worthy of investigation.

Unfortunately, forest rotation period is a difficult measure to define precisely. It is not only influenced by the growth rates of the tree species used in a building, but also by the environment in which the forest exists and the management practices used. To illustrate, Seymour and Hunter (1999) [39] introduced the concept of 'ecological forestry', a modern paradigm of forest management. Under this paradigm, forest management emulates natural pattern of disturbances - such as fires, insect outbreaks, and windstorms - that a forest was subject to prior to human intervention. For example, a 'single-cohort' age structure, referring to a stand where all trees are the same age, is commonly used for aspen forests in the Great Lakes region where severe disturbances cause complete mortality of the forest. Two-cohort age structures are used for forests where severe disturbances do not eliminate the forest but instead leave scattered individuals as 'seed sources'. Examples include scots pine and coastal douglas-fir, and fir-spruce forests of the subboreal region of eastern Canada. In other cases, multi-cohort age structures, like the one shown in Figure 16 below, are used when stand-replacing disturbances are infrequent, but less severe disturbances that remove patches of the forest are more common. Such structures are typically applied to northern hardwood forests in North America.

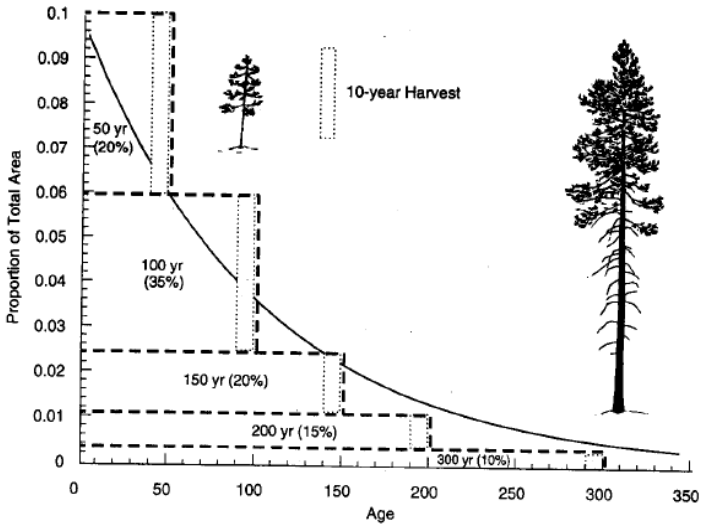

Figure 16: Example of a multi-cohort age structure of a forest stand [39], illustrating complexity in defining the forest rotation period.

The consequence of the complexity of forest management practices means that the wood contained in a mass timber building may be associated with a wide range of rotation periods. Despite this complexity, forestry literature does indicate of typical rotation periods that may be found in the industry. Seymour and Hunter (1999) [39] mentioned a study which found that disturbance frequencies for a wide variety of agents ranged from 0.5% to 2% throughout temperate forests, which corresponds to return intervals of 50-200 years. Bauhus et al. (2009) [40] states that silvicultural practices focused on wood production commonly result in production cycles of 25-150 years. Based on these figures, forest rotation periods of 25, 75, and 200 years are selected for the sensitivity analysis, with 25 and 200 years being extreme values and 75 years being roughly the geometric center. As actual forest rotation periods are unlikely to be exactly any of these values, the only purpose that they serve is to demonstrate the degree of influence that forest growth rate has on the climate impact of a mass timber building. More precise determination of the forest rotation period associated with a building project is recommended as a topic for future research. Figure 17 below shows cumulative growth curves calibrated using the Schnute model [28] for the three chosen rotation periods, and Figure 18 shows the corresponding growth rate curves (equation 15).

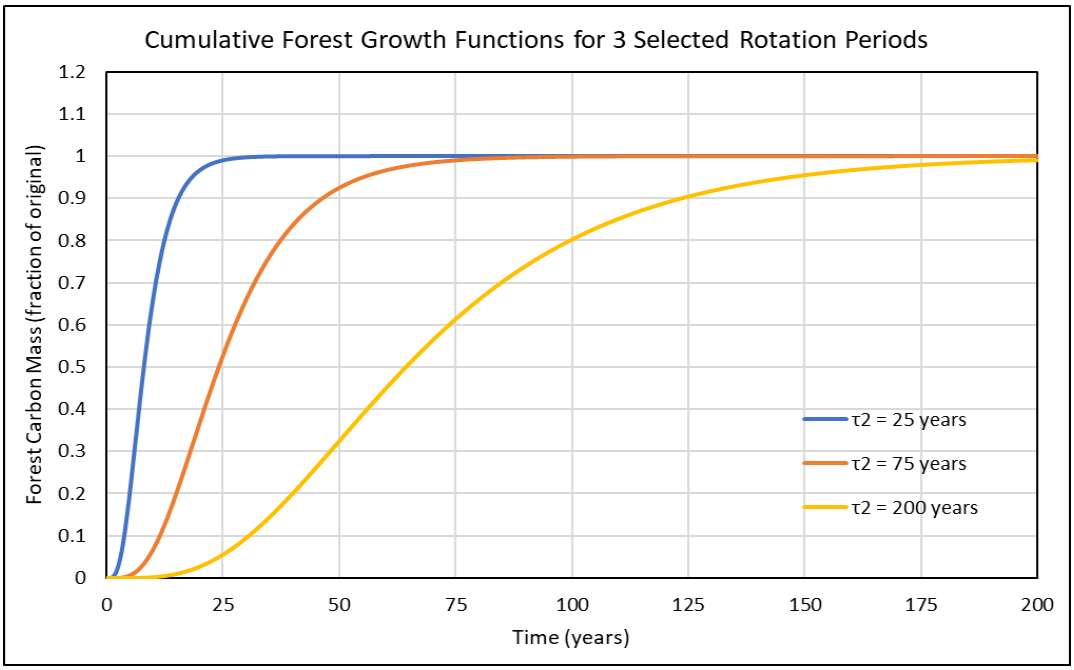

Figure 17: Cumulative forest growth functions created using the Schnute model [28] for rotation periods of 25, 75, and 200 years.

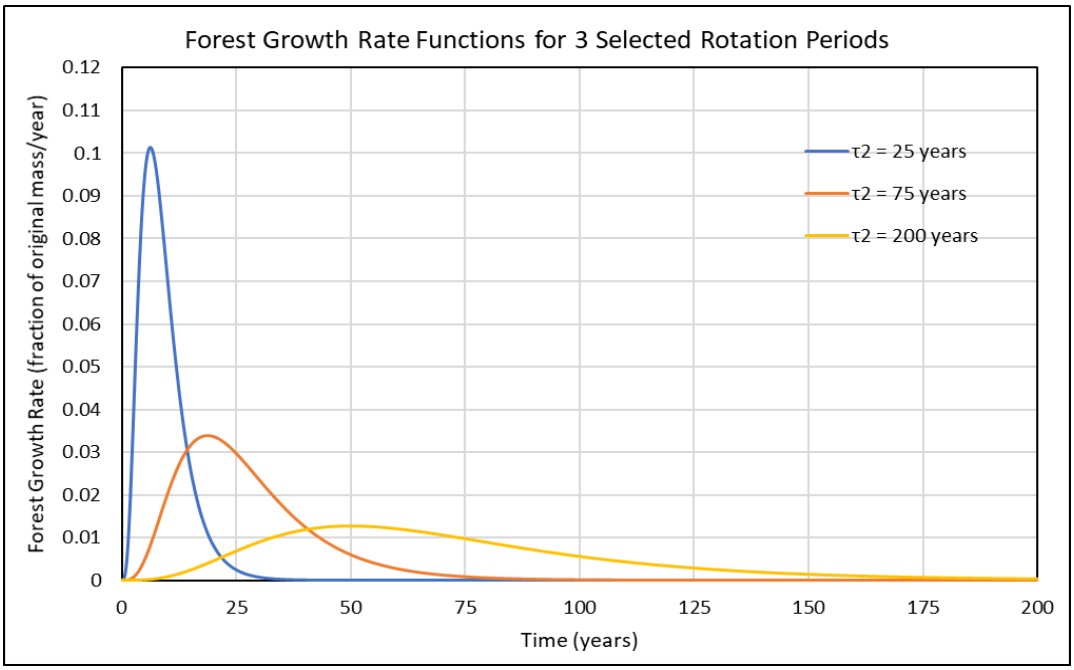

Figure 18: Growth rate-versus-time graphs created using the Schnute model [28] (equation 15) for rotation periods of 25, 75, and 200 years.

Overall, 4 time horizons and 3 forest rotation periods results in a total of 12 scenarios for the sensitivity analysis, shown by Figure 19 below.

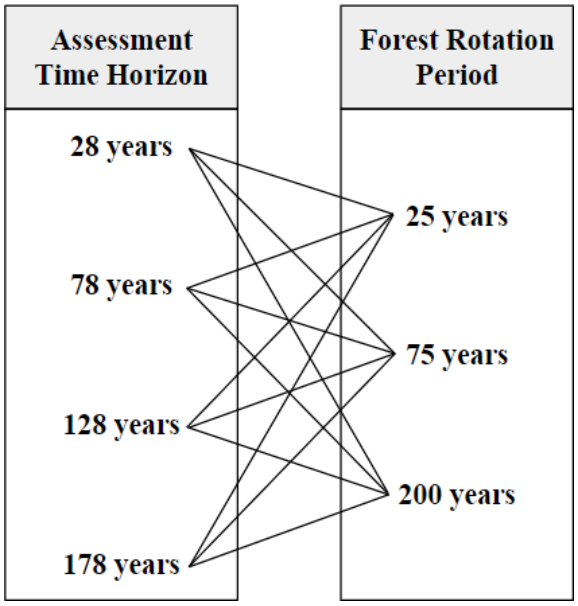

Figure 19: The 12 scenarios, representing all possible combinations of assessment time horizon and forest rotation period, used in the sensitivity analysis.

4.5 Control Variables

The two variables excluded from the sensitivity analysis are the building's lifetime and the treatment scenarios used for woody residues and end-of-life mass timber components. Both of these, however, can significantly affect the climate impact result for a mass timber building. The building's lifetime determines the timing of end-of-life emissions, which influences the temperature change caused by these emissions at the assessment time horizon. Treatment scenarios affect the shape of the building's emission profile. For example, incineration results in pulse emissions at the beginning and end of the building's life, decomposition causes emissions that decay exponentially, while reuse results in no emissions from residue or waste treatment at all. Since the emission profile defines the time distribution of emissions, treatment methods would therefore also affect the climate outcomes. However, to enable greater depth of analysis, these two variables have been left for future research. The following subsections explain the selected values for the control variables.

4.5.1 Building Lifetime

The original study by Chen et al. (2020) [35] estimated the environmental impacts of the case study building over a period of 60 years. Several other LCA studies on mass timber buildings used lifetimes of 50 [15], 60 [41], and 80 years [42]. From a survey of the service lives of North American buildings by O'Connor (2004) [43] the average age of demolished wooden buildings was found to be around 62.7 years. According to the Mass Timber Institute [5], the lifetimes of the structural components of a mass timber building ranges from 50-300 years. Based on these figures, a building lifetime of 60 years, consistent with the original study, is used. This lifetime conforms to the requirement of CSA Standard S478:19 - Durability in buildings that the design service life of 'Long life' buildings like multi-unit residential and mid- and high-rise commercial and office buildings should range from 50 to 99 years [44].

4.5.2 Residue and Waste Treatment Scenarios

A large variety of treatment methods for forest, sawmill, and mass timber production residues are used in industry. For forest residues, the most common treatment method is pile burning [45]. Other possibilities include piling without burning, chipping, creating biochar, or doing nothing to allow the residues to decay aerobically [45]. For sawmill residues, bark and sawdust are typically

sold or used as fuel, while wood chips are usually sold to pump mills [46]. In a mass timber manufacturing plant, internally generated residue, or 'hogfuel', can be used for energy or transferred as waste [9]. Unfortunately, due to the wide range of residue treatment possibilities and the fact that the methods used depend on the logger, sawmill operator, and manufacturing plant, it is difficult to determine the actual combination of residue treatment methods used in a project. For simplicity it is assumed that 50% of all three types of woody residues are burned, while 50% are left to decay aerobically.

Modelling the aerobic decay of residues requires knowing the characteristic time of decay, τ (see equation 14). Wagener and Offord (1972 [34]) studied the decay rate of slash piles in 2 forest stands in Northern California and reported that on average, the test piles reduced in volume by 60-70% over 29 years. This corresponds to a characteristic time of approximately 27.6 years. Spaulding and Hansbrough (1944) [47] reported decay half-lives of 17 years for red spruce slash and 6-8 years for slash from hardwoods and eastern white pine in the Northeastern US. Childs (1939) found that 90% of the volume of douglas-fir slash in the Pacific Northwest decayed 16-20 years after logging, which corresponds to a characteristic time between 7 and 8.7 years. Despite the wide range of reported values, $\tau = 10$ years is used in this study. More accurately estimating the characteristic time of aerobic decay is recommended for future research. Sawmill and mass timber manufacturing residues are assumed to decay at the same rate as forest slash.

Waste treatment scenarios for used mass timber components can be equally difficult to determine. Because mass timber buildings are relatively new, it may be many decades before the first ones reach the end of their lives. Nonetheless, Panojevic and Svensson (2013) [36] mentioned that end-of-life scenarios for CLT involve combinations of 1) landfill, 2) incineration with or without energy recovery, and 3) reuse, either in the components' existing forms or converted into alternative products. Based on these possibilities, like with residues, it is assumed that 50% of all used mass timber components are incinerated, and 50% are sent to landfill.

Regarding the landfill method, Micales and Skog (1997) [33] indicated that while the decomposition of forest products in landfills releases both CO_2 and CH_4, a significant portion of the CO_2 emitted is dissolved into landfill leachate before it could escape into the atmosphere. It is therefore assumed the landfill scenario only releases CH_4. The study [33] also discussed

several types of models for methane production from landfills: zero-order models where CH_4 formation is constant with time, first order models where the rate of CH_4 production decays exponentially with time, and second-order models that are based on the chemistry and microbiology of methane synthesis. A zero-order model was not selected since the study [33] mentioned that it produced unreliable results compared to the other two types. Further, according to Rafey and Siddiqui (2021) [48], although the modelling procedure is more complex for second order approaches, they do not produce corresponding increases in accuracy. As a first-order model appears to be the most preferable, methane emissions from landfill decomposition are modeled using the negative exponential function (equation 14).

Constructing the emission function for landfill decomposition requires knowing both the methane potential of wood, which is the fraction of its carbon mass that is emitted as CH_4 (the rest remains indefinitely in landfill), and the characteristic time of decay, τ. [33] estimates that the maximum methane potential of landfilled wood is about 0.019, or 1.9%. The IPCC, in its 2019 Refinement to the 2006 Guidelines for National Greenhouse Gas Inventories [49] provides decay half-lives for 'Wood/straw waste' as 35 years under 'Dry' conditions and 23 years under 'Wet' conditions. Using an intermediate half-life of 30 years results in $\tau = 43.3$ years. However, both the methane potential of wood and its decay rate is affected by a multitude of factors. According to [33], some factors that influence decomposition rate include the size of waste particles, the composition of waste, and the availability of moisture and nutrients, and some that affect wood's methane potential include moisture level, the presence of toxic chemicals that inhibit bacterial growth, and whether CH_4 is converted to CO_2 through flaring. More accurately determining wood's methane potential as well as the actual emission function associated with landfill decay are also recommended as topics for future research.

4.6 Methodology

The specific version of the proposed LCA method for mass timber buildings detailed in Appendix B is applied to each of the 12 analysis scenarios (see Figure 19) to calculate AGTP values at their respective time horizons. A sample calculation for the scenario with a 78-year time horizon and a forest rotation period of 75 years is provided in Appendix C. AGTP results of the 12 scenarios are then compared in section 5.2.1 to analyze the sensitivity of climate impact of the case study building to the two variables of interest.

The proposed LCA method uses the AGTP, while the original study [35], which uses traditional LCA, expresses climate impacts using the GWP. To enable comparison, the original study's GWP result was converted to an AGTP value. Since the GWP equates all GHG emissions to pulse CO_2 emissions occurring at year 0 by considering their cumulative radiative forcing over 100 years (see equation 1), the conversion is done by multiplying the GWP value, stated in section 4.3 as 4.767×10^5 $kgCO_2e$, by the AGTP of 1 kg of CO_2 emitted as a pulse (delta function) for a time horizon of 100 years, 0.4873×10^{-6} nK from Table 2 in Appendix A. The result is an AGTP of 0.232 nK.

It should be noted that the process of first computing a GWP and then converting it to an AGTP is strongly discouraged. As discussed, the climate impact of an emission depends on its timing relative to the assessment time horizon. The computation of the GWP, however, treats all emissions as occurring at year 0 and imposes a strict time horizon of 100 years. Thus, when the conversion factor is applied to the GWP, the resulting AGTP value will differ from that computed using the actual emission profile of a building and the chosen time horizon. The conversion is only done in this study to compare the result of accounting for the effect of time versus not doing so, and should not be carried out in practice.

5 Results

5.1 Climate Impacts of Unit Emissions and Sequestrations

Figures 20 and 21 below show the time evolution of the AGTP of 1 kg pulse emissions of CO_2 and CH_4, respectively. For example, as Figure 20 shows, 25 years after a pulse CO_2 emission, the global surface temperature is approximately 0.65×10^{-6} nanokelvins (nK) higher relative to that at year 0. 150 years after the emission, it is about 0.47×10^{-6} nK higher. The reason for the initial temperature peak followed by gradual cooling can be seen from the negative exponential nature of the IRF of surface temperature to radiative forcing (equation 11). According to the Bern CC model (equation 2), radiative forcing caused by a pulse CO_2 emission is highest immediately after the emission, and decays exponentially (see red curve in Figure 20). As such, the peak AGTP, which is caused by the initial high radiative forcing, occurs close to year 0. However, as shown by equation 11, the impact of radiative forcing on surface temperature decays with time. By year 150, the effect of the initial high radiative forcing would have diminished, hence the decrease in AGTP relative to year 25.

The AGTP curve of a 1 kg pulse emission of CH_4, shown in Figure 21, exhibits a similar pattern, with an initial peak followed by a period of decrease. This is because like CO_2, the IRF of CH_4 (equation 4) also decays with time, as shown by the red curve in Figure 21. However, unlike CO_2, the AGTP of methane asymptotically approaches 0. This is because its radiative forcing decays to 0, while that of CO_2 does not. The AGTP of a pulse CH_4 emission becomes negligible compared to its peak after about 75 years (around 6 perturbation lifetimes), while the AGTP of CO_2 remains significant long after the emission. Furthermore, for time horizons greater than about 100 years, as both Figures 20 and 21 show, the AGTP of both CO_2 and CH_4 become more-or-less stable with time.

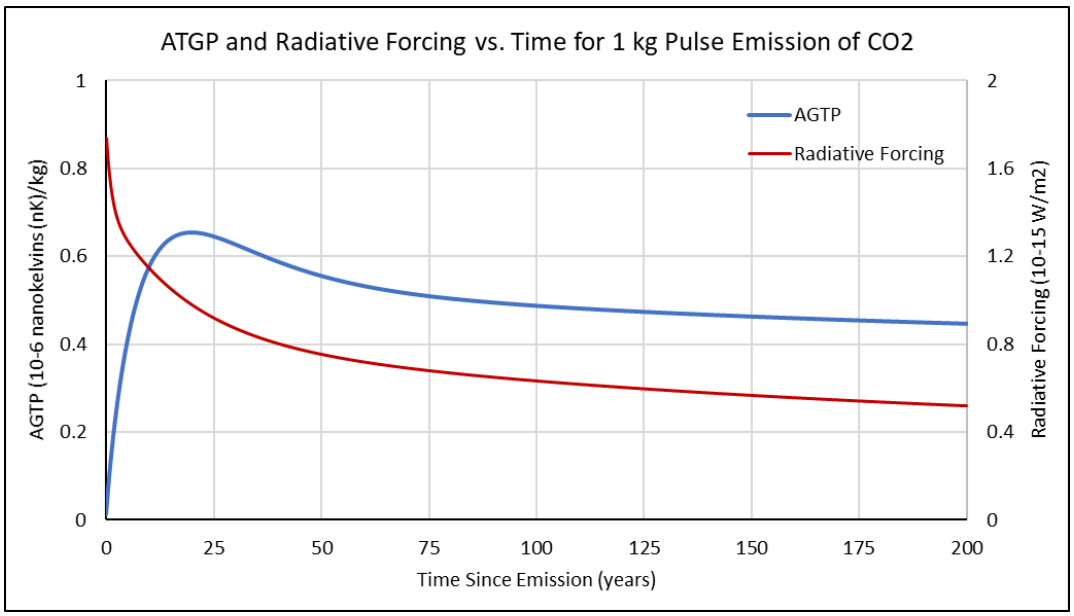

Figure 20: AGTP versus time graph and radiative forcing profile of a 1 kg pulse CO_2 emission.

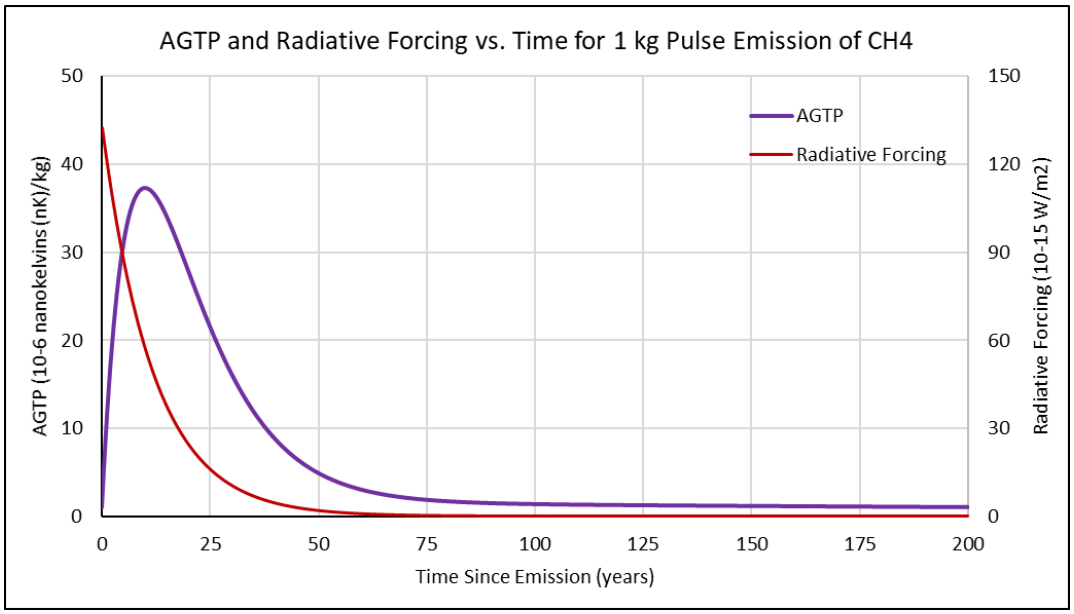

Figure 21: AGTP versus time graph and radiative forcing profile of a 1 kg pulse CH_4 emission.

The above two figures validate the fact that the climate impact of an GHG emission depends on the time horizon at which it is analyzed. For example, from Figure 21, the AGTP of a 1 kg pulse CH_4 emission is approximately 37×10^{-6} nK when using a 10-year time horizon, but decreases to only $\cong 5 \times 10^{-6}$ nK at year 50. Due to this time dependence, the traditional LCA approach of adding emissions regardless of their timing will not produce their true climate impact at any

point in time. A possible exception is when climate impacts are being analyzed at very long time horizons because, as mentioned, the AGTP of pulse emissions of both CO_2 and CH_4 stabilize after about 100 years. However very long time horizons are not relevant to climate policies that are concerned with impact on timescales of several decades.

Figure 22 below shows the time evolution of the AGTP of 1 kg CO_2 emissions distributed according to the negative exponential function (equation 14), for values of τ ranging from 5 to 50 years. The curve for a 1 kg pulse CO_2 emission is plotted in red for comparison. Figure 23 below similarly shows AGTP curves for 1 kg CH_4 emissions distributed according to the negative exponential function with τ ranging from 5 to 50 years. For small values of τ, AGTP curves of distributed CO_2 and CH_4 emission are similar to those of pulse emissions. This is because the delta function, $\delta(t)$, is the limiting case of a negative exponential function as τ approaches 0. As τ increases, the peak AGTP of both gases decrease in magnitude and shift forward in time. For CO_2, it almost disappears for $\tau \gtrsim 25$ years. Reduction in peak AGTP occurs because when emissions are more spread out in time, their initial peak RF is smaller.

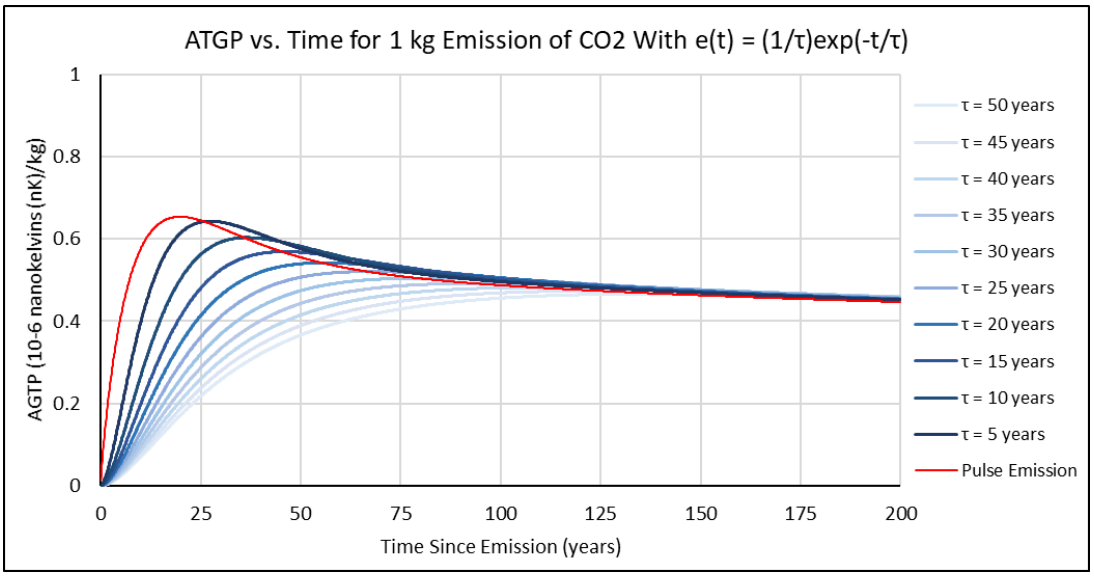

Figure 22: AGTP versus time graphs of 1 kg distributed CO_2 emissions following the negative exponential emission function (equation 14), for various values of τ.

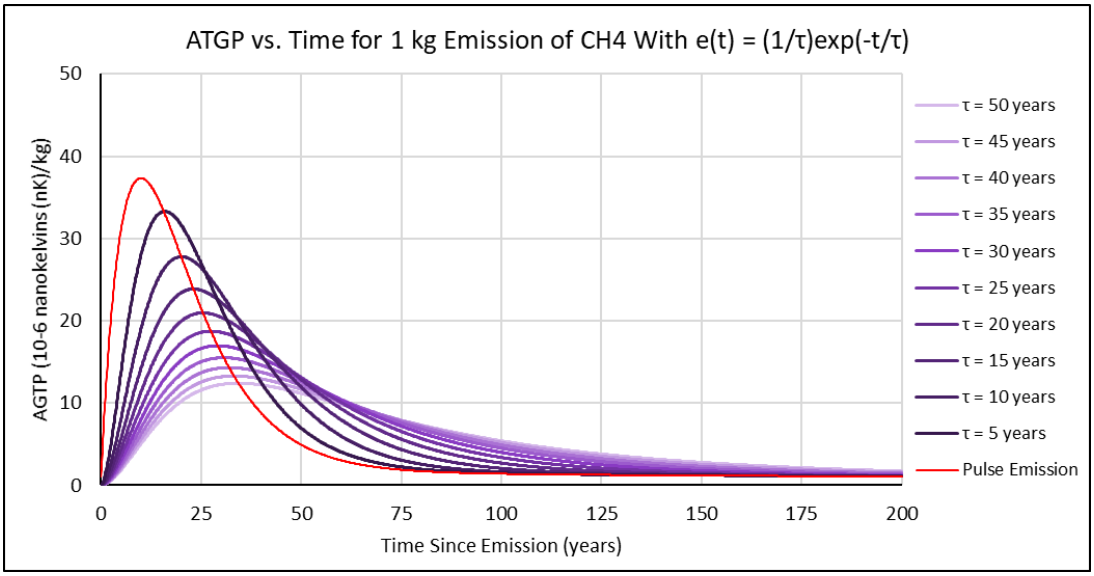

Figure 23: AGTP versus time graphs of 1 kg distributed CH_4 emissions following the negative exponential emission function (equation 14), for various values of τ.

A key takeaway from the above two figures is that the climate impact of a GHG emission not only depends on its time of initiation, but also on how it is distributed. As shown by Figure 23, the AGTP curve of CH_4 for τ = 5 years is very different from that for τ = 50 years. This further highlights the inadequacy of traditional LCA, which ignores the time-distribution of emissions. A notable observation, however, is that for both gases, at time horizons of about 125 years or longer, AGTP curves for all values of τ converge to those of pulse emissions. Thus, if the assessment time horizon is around 125 years or more longer than the building's lifetime, it might be acceptable to approximate all emissions as pulses. Nonetheless, the relevance of such long time horizons to current climate policies might be questionable. Finally, as with pulse emissions, the AGTP curves of distributed emissions of both gases for all values of τ become relatively stable with time after about 125 years.

Figure 24 shows AGTP versus time curves for 1 kg CO_2 removals by forest growth following the Schnute growth function (equation 15), for rotation periods r ranging from 25 to 200 years. The AGTP curve for an instantaneous or 'pulse' removal is plotted for comparison.

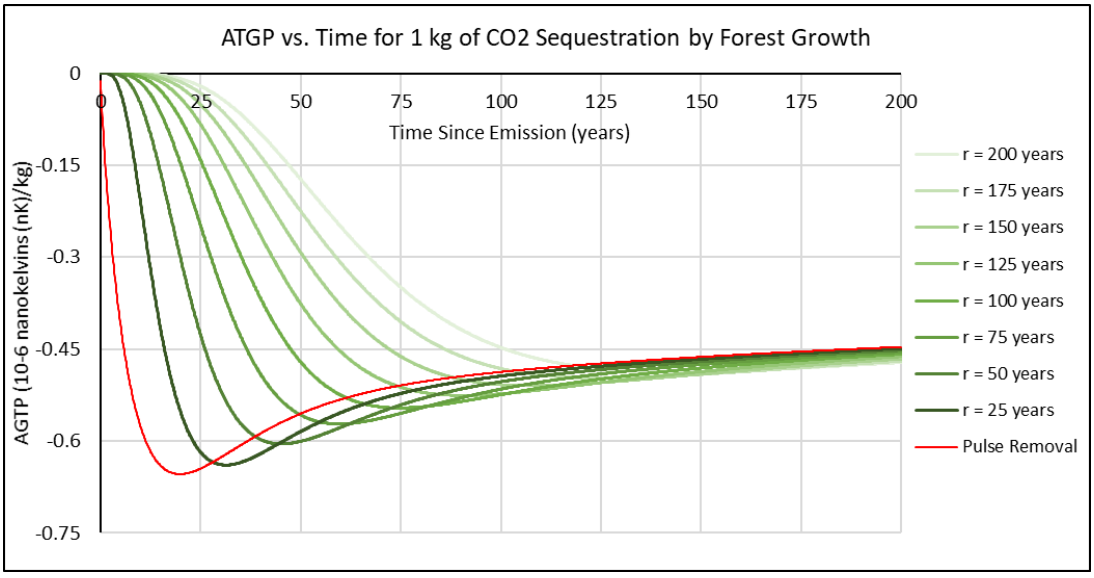

Figure 24: AGTP versus time graphs of 1 kg CO_2 removals by forest growth modeled using the Schnute growth function for various forest rotation periods, *r*.

This graph shows that like with CO_2 emissions, the time-distribution of CO_2 sequestration is a strong determinant of its climate impact, and that such impact depends on the assessment time horizon. For example, at year 50, a forest stand with r = 25 years would result in a much larger AGTP reduction than one with r = 200 years, even if both stands eventually absorb the same amount of CO_2. Again, this observation supports the argument that in general, carbon flows distributed in different ways should not be added together equal weighting. Finally, as with the AGTP curves shown in Figures 22 and 23 for emissions, all 8 curves for forest growth converge to that of the pulse removal and stabilize with time at after around 125 years.

5.2 Results of the Sensitivity Analysis

5.2.1 Scenario Analysis

Figure 25 below compares the AGTP of the case study building under the 12 analysis scenarios (see Figure 19). For example, in the scenario with a 28-year time horizon (TH) (representing the year 2050) and a rotation period of 200 years, the AGTP of the building is approximately 2.1 nK, while in the scenario with TH = 178 years (representing year 2200) and r = 75 years, its AGTP is about 0.3 nK.

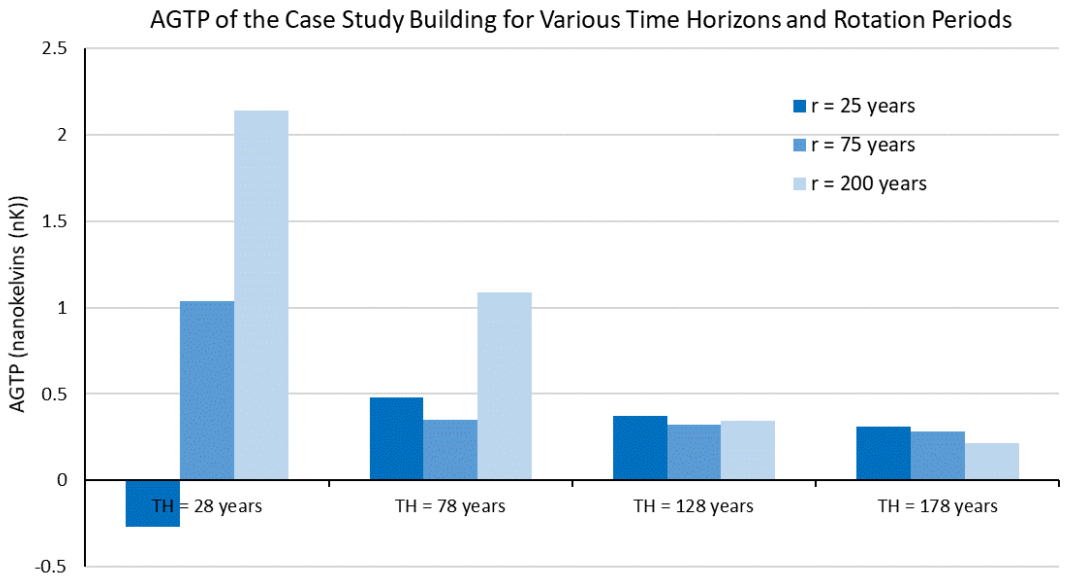

Figure 25: AGTP of the case study building at time horizons of 28, 78, 128, and 178 years for forest rotation periods of 25, 75, and 200 years.

Figure 25 shows that firstly, the climate impact of a mass timber building depends on forest rotation period. Sensitivity is pronounced at short time horizons, as seen from the large differences between the three column heights at TH = 28 years. To explain these differences, at year 28, a forest stand with r = 25 years would have already reached its mature size. As shown by Figure 24, the AGTP curve of CO_2 sequestration with r = 25 years reaches minimum at around this time. The total AGTP of the building is negative in this scenario since the AGTP reduction caused by forest regrowth exceeds the positive AGTP contributions by MTC and residue treatment emissions. However, at year 28, a forest stand with r = 75 years would still be in its accelerated growth phase. Figure 24 shows that the AGTP curve of CO_2 sequestration with r = 75 years has not yet reached its minimum at year 28. As AGTP contributions by MTC and residue emissions exceed AGTP reductions by forest growth, the building's total AGTP is positive in this scenario. Similarly, as Figure 24 shows, the AGTP curve of a forest with r = 200 years is still very low at year 28. Since positive AGTP contributions far exceed AGTP reductions by forest growth in the scenario with r = 200 years, the total AGTP of the building is highly positive at around 2.1 nK.

Despite significant sensitivity to forest rotation period existing at TH = 28 years and TH = 78 years, this sensitivity diminishes at TH = 128 years and TH = 178 years. As Figure 25 shows,

column heights of the 3 growth cases at both of the latter two time horizons are similar. This observation can also be explained by examining Figure 24. As it shows, the AGTP curves associated with all 3 rotation periods take on nearly the same value after about 125 years. Since the temperature reduction by forest growth is similar for all three rotation periods at long time horizons, the total AGTP of all 6 scenarios with TH = 128 years and TH = 178 years are similar. Thus, it can be concluded that while a mass timber's global warming impact is sensitive to forest rotation period at short time horizons less than about 125 years, it is not sensitive to forest rotation period at longer time horizons.

Figure 25 further shows that secondly, the climate impact of a mass timber building is sensitive to the assessment time horizon. This is apparent when comparing column heights at TH = 28 years to those at TH = 78 years. A major difference between the two time horizons is that while the former occurs before the building's end-of-life stage at year 60, the latter occurs afterwards. The AGTP contribution of end-of-life emissions is thus accounted for in the scenarios with TH = 78 years, but not in those with TH = 28 years. The impact of this difference is apparent in the jump in the AGTP of the r = 25 years forest growth case from being negative at TH = 28 years to being positive at TH = 78 years. Note that the AGTPs of the r = 75 years and r = 200 years growth cases still decreased from TH = 28 years to TH = 78 years because in these cases, the increase in AGTP reduction by forest growth from year 28 to year 78 exceed the AGTP contribution of end-of-life emissions. Overall, using time horizons shorter than the building's lifespan produces incomplete climate results by neglecting the end-of-life stage. The LCA practitioner should ensure that the use of such short time horizons align with the goals of the LCA, and interpret results with care when life cycle stages are excluded from the study.

Moreover, it can be seen from Figure 25 that the AGTP of all 3 forest growth cases do not differ significantly from TH = 128 years to TH = 178 years, indicating loss of sensitivity to the time of assessment at such long time horizons. This is because as noted previously, AGTP curves for all emissions functions eventually become relatively stable with time after approximately 100-125 years. Thus, for the case study building, selecting a time horizon longer than 128 years is not warranted as it would not result in more accurate climate impacts, but would decrease the relevance of the results to climate policies.

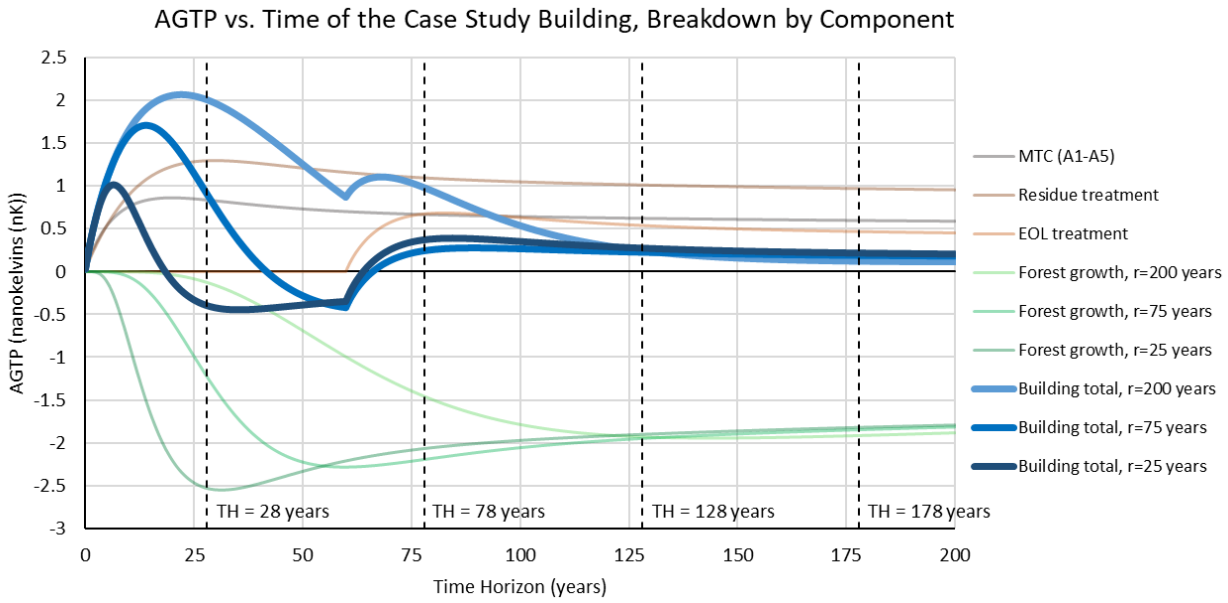

Figure 26: AGTP-versus-time graphs of the case study building under 3 forest growth cases, as well as of the 4 main life cycle stages included in the LCA: MTC, residue treatment, end-of-life waste treatment, and forest growth.

Figure 26 shows how the AGTP of the case study building evolves continuously with time under the 3 studied forest rotation periods (the blue lines). It also shows the AGTP graphs associated with the 4 life cycle stages included in the LCA (see section 4.3), with the grey line representing MTC emissions, the brown lines representing residue and end-of-life treatment emissions, and the green lines representing forest growth with rotation periods of 25, 75, and 200 years. The light blue curve is the AGTP-versus-time graph of the building for a 200-year rotation period, and is the superposition of the 'MTC', 'Residue treatment', 'EOL treatment' and 'Forest growth, r=200 years' curves. Similarly, the medium blue curve is the AGTP-versus-time graph for a 75-year rotation period, and the dark blue curve is that for a 25-year rotation period.

All three AGTP curves exhibit an initial peak followed by a period of rapid decrease. This is because while beginning-of-life emissions, including those from MTC and residue treatment, mostly occur instantaneously, carbon uptake by forest growth is highly distributed over time. Shortly after building construction, the effects MTC and residue treatment emissions dominate the AGTP of the building. Acceleration of forest growth then causes the AGTP curve to peak and then decline. The magnitude of the peak is small for shorter rotation periods as faster forest

growth enables the effects of carbon sequestration to more quickly 'catch-up' with the those of MTC and residue treatment emissions. As the AGTP curves under both the 25-years and 75-year rotation periods drop below zero, it means that interestingly, in both cases, the building's climate impact is a net cooling effect for a portion of its life. The AGTP of the building suddenly rises at year 60 under all three rotation periods as the building reaches its end-of-life, and its wooden components release carbon through incineration and landfill decomposition. Because of this, although the r = 25 years and r = 75 years scenarios temporarily resulted in global cooling, their long-term global warming impacts are still positive. After around 125 years, the AGTP curves under all three forest rotation periods converge. Consistent with Figure 25, this shows that at long time horizons, a mass timber building's AGTP is not sensitive to either the forest rotation period or the time of assessment.

5.2.2 Comparison with the Original Study

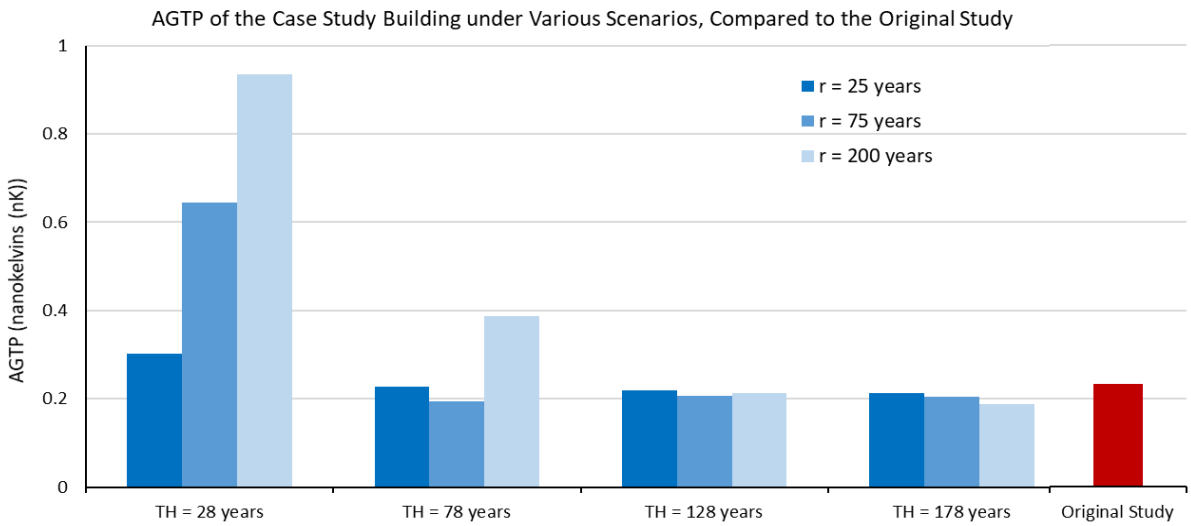

Figure 27: AGTP of the case study building under the 12 analysis scenarios compared to the result of the original study by Chen et al. (2020) [35].

Figure 27 above compares the AGTP of the 12 analysis scenarios, calculated using the proposed LCA method, to the result of the original study by Chen et al. (2020) [35], which used traditional LCA. The original study did not account for biogenic emissions from residue or EOL treatment and assumed that the forest only uptakes 1.05×10^6 kg of CO_2 instead of the 3.99×10^6 kg computed in this study (see Appendix C). The reasons are unexplained. Nonetheless, to limit the

comparison to highlighting the differences between capturing time versus not doing so, the present study's calculations were modified to match the original one. This is why the blue columns in Figure 27 are different from those in Figure 25. The method used to convert the original study's GWP result to an AGTP value was described in section 4.6. Note again that this conversion should not be done in practice because the calculation of a GWP implicitly neglects timing differences and imposes a strict time horizon of 100 years.

Figure 27 shows that three analysis scenarios significantly exceeded the original study's results: r = 75 years at TH = 28 years, r = 200 years at TH = 28 years, and r = 200 years at TH = 78 years. All three scenarios can be described as having short time horizons and long rotation periods. The reason for this is that while traditional LCA assumes that both MTC emissions and CO_2 sequestration occur instantaneously at year 0, the reality is that the former occurs much sooner than the latter because forest growth is slow compared to manufacturing processes. At short time horizons, the positive AGTP contribution by MTC emissions exceeds the AGTP reduction by forest growth. The proposed LCA method captures the effect of this timing difference while traditional LCA does not, hence why the AGTP of these three analysis scenarios are higher than that of the original study.

Interestingly, however, all analysis scenarios with TH = 128 years and TH = 178 years produced similar AGTP values as the original study. The likely explanation is that, as observed from Figures 22, 23, and 24, at time horizons as long as 128 or 178 years, the effect of varying the time-distribution of carbon flows diminish. The AGTP curves of all distributed flows, no matter which gas is emitted or removed and which emission function is followed, all converge to those of their respective pulse events. It could therefore be concluded that at time horizons longer than around 125 years, the combined effects of the distributed emissions in a building's life cycle may be reasonably approximated by treating those emissions as pulses occurring at year 0, like in a traditional LCA.

6 Discussion

6.1 General Remarks

Figures 20 to 24 showed that the climate impact of a GHG emission or removal both depends on how it is distributed over time, and changes with the time at which it is evaluated. Because of this, the AGTP of a mass timber building is, in general, sensitive to both forest rotation period and the assessment time horizon. Although long-term impacts have limited dependence on forest rotation period, in the short term, buildings built with wood from short-rotation stands have lower impact. Similarly, although the building's AGTP in all forest growth cases stabilize at long time horizons, they vary greatly in the near term since shorter time horizons give greater emphasis to the timing differences between carbon flows. Consequently, both forest rotation period and assessment time horizon are crucial factors to consider when comparing mass timber and conventional buildings from a climate standpoint.

A key conclusion drawn from comparing results between the present and original studies, as well as from Figure 26, is that the climate impact of a building - or of any product system in general - evolves organically over time as the atmosphere, ocean, and land ecosystems respond to and absorb perturbations in the Earth's radiation balance. Advanced LCA methods that account for time can capture this behavior, while traditional LCA presents climate impact in an unrealistic manner as a static, unchanging value. The ability to more accurately reflect nature in a general sense supports the need for advanced LCA methods.

Comparing the present study's results to that of the original one, it was observed that for scenarios with long time horizons or short forest rotation periods, AGTP results were similar to those obtained using traditional LCA. The fact that the AGTPs of distributed emissions and removals converge to those of pulse events at long time horizons means that when computing long-term surface temperature impacts, it may be acceptable to treat all carbon flows as pulses occurring at year 0. This conclusion reflects the statement made in section 1 that the traditional LCA approach of giving equal weighting to time may be acceptable when the time horizon of interest is much longer than a typical building's lifespan. However, to more accurately capture short-term climate impacts that are of greater interest to current climate policies, advanced LCA methods are still necessary.

6.2 Strengths and Weaknesses of the Proposed Method

The strengths of the LCA method proposed in section 3 include its use of a relevant impact metric, the AGTP, and its support for a consistent time horizon. Like the GWP_{bio}, the proposed method achieves low data and computational demand by using simple emission functions to approximate complex emission profiles. Instead of evaluating emission quantities for a large number of timesteps, the LCA practitioner only needs to determine the most significant emission events in a building's life cycle and assess how those emissions are distributed over time. A relatively low level of expertise is needed to do this, especially if guidance can be provided by an LCA standard. Sophisticated software modelling is not required since the equations used (see Appendix B) are simple and can be evaluated with a spreadsheet. Furthermore, by using multiple emission functions to model the emission profile instead of a single PDF, the proposed method improves upon the accuracy of the GWP_{bio} method. These strengths make the proposed method a suitable candidate for use by building designers in evaluating material and design choices from a climate perspective at the early design stage.

The proposed LCA method has several weaknesses, some of which are shared with GWP_{bio}. Firstly, like GWP_{bio}, the proposed method assumes that the forest stand will completely regenerate. As mentioned, this may not occur due to a variety of factors [19]. Secondly, although using multiple emission functions improves the accuracy of results compared to GWP_{bio}, these simple functions are still rough approximations of the actual time-distributions of carbon flows associated with emission events. For example, although the negative exponential function approximates emissions from decomposition of forest residues, the actual emission-versus-time graph may deviate from this function for many reasons. The rate of decay may slow down due to a dry summer or speed up after a wet one. Likewise, disturbances like fires may end the decay process abruptly. Approximation errors associated with emission functions is an inherent source of uncertainty associated with the proposed method.

Finally, using the AGTP as the impact metric creates another inherent source of error. As mentioned by Shine et al. (2005) [30], while metrics that are further down in the cause-and-effect chain associated with GHG emissions (see Figure 12) are more relevant, they are also subject to greater uncertainty. The global warming potential inherits uncertainty from the Bern CC model (equation 2). The AGTP contains this source of error too, but also inherits uncertainty from the

IRF of surface temperature to radiative forcing (equation 11). This IRF was taken from a single study [31], and does not appear to be recognized by large organizations like the IPCC. Although further research may improve the accuracy of this function and that of the Bern CC model, the use of a more relevant impact metric will always come at the expense of greater uncertainty.

6.3 Practicality of the Proposed LCA Method for Standardization

The proposed LCA method is suitable for adoption by LCA standards due to its simplicity and ability to be formulated as a step-by-step procedure (see Appendix B). Despite this, results obtained using it are subject to several sources of uncertainty in addition to the inherent ones associated with emission functions and the AGTP. This section describes three of these sources. Should the proposed method become standardized, the LCA standard should, with future research, provide guidance to the LCA practitioner on addressing these uncertainties.

1. Forest growth: rotation period, growth function, sustainability, and baseline scenario

As mentioned in section 4.4.2, it is difficult to precisely define a forest rotation period for a mass timber building. Forest rotation period depends on tree species, the natural disturbance regime present, and the management practices of those with authority over the forest. Multiple rotation periods may exist concurrently if a stand is managed with a complex age structure like that shown in Figure 16. As shown by the sensitivity analysis, the short-term AGTP of a mass timber building is strongly influenced by the rate of forest growth. Thus, the LCA standard should provide guidance on the appropriate selection of a forest rotation period.

Additionally, as discussed in section 3.2, the forest growth function (equation 15) used to compute AGTP factors for carbon sequestration was not calibrated using empirical data. The decision for the Schnute growth function (equation 15) to take on an ‘S’-shape, exhibit an inflection point at ¼ of the forest rotation period, and to reach 99% of its asymptotic value at the rotation period were made arbitrarily. Erroneous results would occur if this function does not reflect real-life forest growth. To minimize such error, equation 15 should be calibrated using field data on the actual growth patterns exhibited by forests.

Moreover, as discussed, the proposed method assumes that the forest stand will completely regenerate, which may not happen for a variety of reasons [19]. In instances where the forest

fails to regrow, the building should not be credited with the full AGTP reduction of carbon sequestration. To address this, the LCA standard could require that the AGTP reduction by forest growth can only be claimed if it can be proven, for example using forest sustainability certifications, that the forest stand from which raw materials were extracted is managed sustainably and has a very high likelihood of regeneration.

Furthermore, the LCA standard should consider the issue of selecting a 'baseline' scenario for forest growth. As mentioned in section 1, 2 of the 3 prominent viewpoints on the climate impact of timber construction are 1) that wood use is positive for the climate due to CO_2 sequestration, and 2) that wood use is detrimental since bioCO_2 emissions occur sooner than forest regrowth. Both are based on giving greater importance to earlier emissions than later ones. However, a key difference is that while the former uses a baseline scenario where the forest stand did not previously exist - effectively giving an 'afforestation credit' to the building - the latter uses one where one already exists. The proposed method follows the latter assumption, modelling forest regrowth as beginning at year 0. If the former assumption is used, however, climate impact results would be significantly different since the green curves shown in Figure 26 would shift an entire forest rotation period backwards in time. The LCA standard should therefore provide guidance on whether to select a baseline scenario without a pre-existing forest, or one where the forest is already established.

2. Building lifetime

The lifetime of a building determines the timing of its end-of-life stage relative to the assessment time horizon, and thus the climate impacts of end-of-life emissions. As shown by Figure 26, end-of-life emissions can contribute significantly to a mass timber building's total AGTP. However, a building's lifetime is typically unknown at the design stage. The 60-year lifetime used in this study, discussed in section 4.5.1, came from a limited survey of literature. It is thus recommended for the LCA standard to establish a standard building lifetime following more rigorous research in order to enable comparison between LCA studies.

3. Residue and end-of-life treatment methods

As discussed in section 4.5.2, the sensitivity analysis assumed that 50% of forest, lumber production, and mass timber manufacturing residues as well as end-of-life mass timber

components are incinerated, while 50% are left to decay - aerobically in nature to produce CO_2 in the case of residues, and anaerobically in landfill to produce CH_4 in the case of used mass timber components. In real life, treatment methods used for residues strongly depend on the choices of the logger, the sawmill, and the mass timber manufacturing plant. Likewise, the end-of-life scenario of a mass timber building is not limited to incineration and landfill. For example, some used components may be reused in their original forms, and some may be re-manufactured into different wood products [36]. The building may also be refurbished to serve a different function. As different treatment scenarios have different emission functions, the choice of residue and waste treatment option strongly influences a mass timber building's AGTP. Therefore, the LCA standard should provide instructions on how to most appropriately select a combination of treatment methods for a particular project.

In addition to resolving these uncertainties, the LCA standard should also establish a standard assessment time horizon to enable comparability between studies. The choice of time horizon has significant implications on the type of climate impact analyzed. Choosing a time horizon of 125 years or longer is relevant when long term impacts, such as whether or not global warming will exceed the Paris Agreement targets, are of interest. Very long time horizons are unnecessary, however, because as shown by Figures 25 and 26, the climate impact of a mass timber building becomes relatively stable after about 125 years. Meanwhile, a short time horizon like 25 or 50 years should be used when short-term impacts are of interest, for example the degree to which global warming will overshoot the Paris Agreement targets. However, using time horizons shorter than a building's lifespan risks neglecting significant climate impacts by excluding the end-of-life stage. Unfortunately, according to the IPCC, there are currently no scientific, political, or economic bases for choosing a time horizon for assessing anthropogenic interference in the climate system [32]. Thus, establishing a standard time horizon should involve both scientific research as well as policy and economic analyses.

7 Conclusion

The climate implication of the transition to mass timber buildings is a highly contentious issue. Despite a lack of accurate climate information, the widespread belief that wood is more environmentally sustainable than traditional construction materials has led mass timber to proliferate over the past decade. In the face of this growing trend, there is an urgent need for the climate impacts of construction wood products to be examined with greater rigor.

The traditional LCA practice of assigning equal weighting to time is inadequate as it does not capture the fact that the climate impact of an emission both depends on its distribution and on the time of assessment. It is therefore incapable of giving accurate results when a mass timber building's life cycle involves highly distributed carbon flows, such as forest growth. The sensitivity analysis found that the AGTP of a mass timber building depends on both forest rotation period and the assessment time horizon. Traditional LCA cannot capture these dependencies, and instead depicts climate impact as a static, unchanging value. When climate impacts in the distant future are of interest, the traditional method may produce acceptable results. However, to accurately analyze short-term impacts that are more relevant to current climate policies, advanced LCA methods that include the dimension of time are needed.

Based on a literature review of four advanced LCA methods, this thesis proposed a new LCA method that accounts for the effect of time. The proposed method enables a consistent time horizon for impact assessment and uses a highly relevant impact metric, the absolute global temperature change potential. It achieves low data and computational demand by using simple emission functions to approximate the emission profile of a mass timber building, and having tabulated AGTP factors for various emission functions. The proposed method has several weaknesses, however, including reliance on forest regeneration, and inherent errors arising from the approximate nature of emission functions and from the AGTP metric. Nonetheless, its simplicity makes it suitable for inclusion in LCA standards and for use by building designers. Much research is still needed to address several areas of uncertainty discussed in section 6.3, as well as to establish a standard time horizon for impact assessment. Despite this, the proposed method has great potential for supporting climate-based decision-making at the early design stage when the possibility of mitigating embodied emissions is the greatest [1].

Through the sensitivity analysis, this thesis contributes to creating a more complete understanding of the factors that affect the global warming impact of mass timber buildings. To further understand the climate implications of the shift to mass timber, future research should conduct additional analyses using other variables like waste treatment scenario and building lifetime. LCA studies that directly compare mass timber and conventional buildings, like the one conducted by Chen et al. (2020) [35], should also be conducted using advanced LCA methods. Ultimately, as new technologies emerge, the LCA methods used to assess their environmental impacts need to evolve in order to address the new challenges that these technologies bring. It is hoped that this thesis will inspire future research in advanced LCA methods and foster a continuous effort to advance this crucial discipline.

References

[1] World Green Building Council, "Bringing embodied carbon upfront Coordinated action for the building and construction sector to tackle embodied carbon," 2019.

[2] M. Röck, M. R. M. Saade, M. Balouktsi, F. N. Rasmussen, H. Birgisdottir, R. Frischknecht, G. Habert, T. Lützkendorf and A. Passer, "Embodied GHG emissions of buildings – The hidden challenge for effective climate change mitigation," *Applied Energy,* vol. 258, no. 114107, 2020.

[3] J. Cover, "Mass Timber: The New Sustainable Choice for Tall Buildings," *International Journal of High-Rise Buildings,* vol. 9, no. 1, pp. 87-93, 2020.

[4] R. Anderson, D. Atkins, B. Beck, E. Dawson and C. B. Gale, "2020 North American Mass Timber State of the Industry," Forest Business Network, 2020.

[5] T. Kesik and R. Martin, "Mass Timber Building Science Primer," Mass Timber Institute, University of Toronto, Toronto, Canada, 2021.

[6] A. M. Harte, "Mass timber – the emergence of a modern construction material," *Journal of Structural Integrity and Maintenance,* vol. 2, no. 3, pp. 121-132, 2017.

[7] C. X. Chen, F. Pierobon and I. Ganguly, "Life Cycle Assessment (LCA) of Cross-Laminated Timber (CLT) Produced in Western Washington: The Role of Logistics and Wood Species Mix," *Sustainability,* vol. 11, no. 5, p. 1278, 2019.

[8] Athena Sustainable Materials Institute, "A Life Cycle Assessment of Cross-Laminated Timber Produced in Canada," Ottawa, ON, Canada, 2013.

[9] Athena Sustainable Materials Institute, "A Cradle-to-Gate Life Cycle Assessment of Cross-Laminated Timber and Glued-laminated Timber Manufactured by Structurlam," 2019.

[10] M. Puettmann, A. Sinha and I. Ganguly, "LIFE CYCLE ENERGY AND ENVIRONMENTAL IMPACTS OF CROSS LAMINATED TIMBER MADE WITH COASTAL DOUGLAS-FIR," *Journal of Green Building,* vol. 14, no. 4, pp. 17-33, 2019.

[11] Nordic Structures and FPInnovations, "Environmental Product Declaration Nordic X-Lam," 2018.

[12] Canadian Ready Mixed Concrete Association (CRMCA), "CRMCA Member Industry-Wide EPD for Canadian READY-MIXED CONCRETE," 2017.

[13] American Institute of Steel Construction (AISC), "2021," Environmental Product Declaration Fabricated Hot-Rolled Structural Sections.

[14] E. Hoxha, A. Passer, M. R. M. Saade, D. Trigaux, A. Shuttleworth, F. Pittau, K. Allacker and G. Habert, "Biogenic carbon in buildings: a critical overview of LCA methods," *Buildings and Cities,* vol. 1, no. 1, pp. 504-524, 2020.

[15] A. B. Robertson, F. C. F. Lam and R. J. Cole, "A Comparative Cradle-to-Gate Life Cycle Assessment of Mid-Rise Office Building Construction Alternatives: Laminated Timber or Reinforced Concrete," *Buildings,* vol. 2, no. 3, pp. 245-270, 2012.

[16] F. Pierobon, M. Huang, K. Simonen and I. Ganguly, "Environmental benefits of using hybrid CLT structure in midrise non-residential construction: An LCA based comparative case study in the U.S. Pacific Northwest," *Journal of Building Engineering,* vol. 26, no. 100862, 2019.

[17] P. Forster, T. Storelvmo, K. Armour, W. Collins, J. L. Dufresne, D. Frame, D. J. Lunt, T. Mauritsen, M. D. Palmer, M. Watanabe, M. Wild and H. Zhang, "The Earth's Energy Budget, Climate Feedbacks, and Climate Sensitivity. In: Climate Change 2021: The Physical Science Basis. Contribution of Working Group I to the Sixth Assessment Report of the Intergovernmental Panel on Climate Change," Intergovernmental Panel on Climate Change (IPCC), 2021.

[18] M. Brandão, A. Levasseur, M. U. F. Kirschbaun and B. P. Weidema, "Key issues and options in accounting for carbon sequestration and temporary storage in life cycle assessment and carbon footprinting," *The International Journal of Life Cycle Assessment,* vol. 18, no. 1, pp. 230-240, 2012.

[19] P. Leturcq, "GHG displacement factors of harvested wood products: the myth of substitution," *Scientific Reports,* vol. 10, no. 20752, 2020.

[20] C. E. Andersen, F. N. Rasmussen, G. Habert and H. Birgisdóttir, "Embodied GHG Emissions of Wooden Buildings - Challenges of Biogenic Carbon Accounting in Currrent LCA Methods," *Frontiers in Built Environment,* vol. 7, no. 729096, 2021.

[21] A. Levasseur, P. Lesage, M. Margni, L. Deschenes and R. Samson, "Considering Time in LCA: Dynamic LCA and Its Application to Global Warming Impact Assessments," *Environmental Science & Technology,* vol. 44, no. 8, pp. 3169-3174, 2010.

[22] International Standards Organization (ISO), "ISO 21930 Sustainability in buildings and civil engineering works — Core rules for environmental product declarations of construction products and services," 2017.

[23] "Parameters for tuning a simple carbon cycle model," United Nations Framework Convention on Climate Change (UNFCCC), [Online]. Available: https://unfccc.int/resource/brazil/carbon.html.

[24] P. M. Costa and C. Wilson, "AN EQUIVALENCE FACTOR BETWEEN CO2 AVOIDED EMISSIONS AND SEQUESTRATION – DESCRIPTION AND APPLICATIONS IN FORESTRY," *Mitigation and Adaptation Strategies for Global Change,* vol. 5, pp. 51-60, 2000.

[25] P. M. Fearnside, D. A. Lashof and P. Moura-Costa, "ACCOUNTING FOR TIME IN MITIGATING GLOBALWARMING THROUGH LAND-USE CHANGE AND FORESTRY," *Mitigation and Adaptation Strategies for Global Change,* vol. 5, pp. 239-270, 2000.

[26] F. Cherubini, G. P. Peters, T. Berntsen, A. H. Strømman and E. Hertwich, "CO2 emissions from biomass combustion for bioenergy: atmospheric decay and contribution to global warming," *Global Change Biology Bioenergy,* vol. 3, no. 5, pp. 413-426, 2011.

[27] F. Cherubini, G. Guest and A. H. Strømman, "Application of probability distributions to the modeling of biogenic CO2 fluxes in life cycle assessment," *Global Change Biology Bioenergy,* vol. 4, no. 6, pp. 784-798, 2012.

[28] J. Schnute, "A Versatile Growth Model with Statistically Stable Parameters," *Canadian Journal of Fisheries and Aquatic Sciences,* vol. 38, pp. 1128-1140, 1981.

[29] G. P. Peters, B. Aamaas, T. Berntsen and J. S. Fuglestvedt, "The integrated global temperature change potential (iGTP) and relationships between emission metrics," *Environmental Research Letters,* vol. 6, no. 4, 2011.

[30] K. P. Shine, J. S. Fuglestvedt, K. Hailemariam and N. Stuber, "Alternatives to the Global Warming Potential for Comparing Climate Impacts of Emissions of Greenhouse Gases," *Climatic Change,* vol. 68, pp. 281-302, 2005.

[31] O. Boucher and M. S. Reddy, "Climate trade-off between black carbon and carbon dioxide emissions," *Energy Policy,* vol. 36, no. 1, pp. 193-200, 2008.

[32] P. Forster, V. Ramaswamy, P. Artaxo, T. Berntsen, R. Betts, D. W. Fahey, J. Haywood, J. Lean, D. C. Lowe, G. Myhre, J. Nganga, R. Prinn, G. Raga, M. Schulz and R. Van Dorland, "Changes in Atmospheric Constituents and in Radiative Forcing. In: Climate Change 2007: The Physical Science Basis. Contribution of Working Group I to the Fourth Assessment Report of the Intergovernmental Panel on Climate Change," Cambridge University Press, Cambridge, United Kingdom and New York, NY, USA, 2007.

[33] J. A. Micales and K. E. Skog, "The Decomposition of Forest Products in Landfills," *International biodeterioration & Biodegradation,* vol. 39, no. 2-3, pp. 145-158, 1997.

[34] W. W. Wagener and H. R. Offord, "LOGGING SLASH: its breakdown and decay at two forests in northern California," U.S. Department of Agriculture Forest Service, Berkeley, California, USA, 1972.

[35] Z. Chen, H. Gu, R. D. Bergman and S. Liang, "Comparative Life-Cycle Assessment of a High-Rise Mass Timber Building with an Equivalent Reinforced Concrete Alternative Using the Athena Impact Estimator for Buildings," *Sustainability,* vol. 12, no. 11, p. 4708, 2020.

[36] D. Panojevic and E. Svensson, "A Life Cycle Assessment of the Environmental Impacts of Cross-Laminated Timber," Lund University, Sweden, 2019.

[37] The European Committee for Standardization (CEN), "BS EN 15978:2011 Sustainability of construction works. Assessment of environmental performance of buildings. Calculation method," 2011.

[38] Intergovernmental Panel on Climate Change, "Global Warming of 1.5°C," 2018.

[39] R. S. Seymour and M. L. Hunter, Jr, "Chapter 2 Principles of Ecological Forestry," in *Maintaining Biodiversity in Forest Ecosystems*, Cambridge University Press, 1999, pp. 22-61.

[40] J. Bauhus, K. Puettmann and C. Messier, "Silviculture for old-growth attributes," *Forest Ecology and Management,* vol. 258, no. 4, pp. 525-537, 2009.

[41] K. Allan and A. R. Phillips, "Comparative Cradle-to-Grave Life Cycle Assessment of Low and Mid-Rise Mass Timber Buildings with Equivalent Structural Steel Alternatives," *Sustainability,* vol. 13, no. 6, p. 3401, 2021.

[42] H. Gu, S. Liang, F. Pierobon, M. Puettmann, I. Ganguly, C. Chen, R. Pasternack, M. Wishnie, S. Jones and I. Maples, "Mass Timber Building Life Cycle Assessment Methodology for the U.S. Regional Case Studies," *Sustainability,* vol. 13, no. 24, p. 14034, 2021.

[43] J. O'Connor, "Survey on actual service lives for North American buildings," 2004.

[44] Canadian Standards Association (CSA), "CSA S478:19 Durability in buildings," 2019.

[45] A. Grotta, "Don’t want to burn? Other options for treating slash after a timber harvest," Oregon State University, 16 October 2019. [Online]. Available: https://blogs.oregonstate.edu/treetopics/2019/10/16/dont-want-to-burn-other-options-for-treating-slash-after-a-timber-harvest/.

[46] American Wood Council (AWC) and Canadian Wood Council (CWC), "Environmental Product Declaration North American Softwood Lumber," 2020.

[47] P. Spaulding and J. R. Hansbrough, "Decay of Logging Slash in the Northeast," U.S. Department of Agriculture, Washington, D.C., 1944.

[48] A. Rafey and F. Z. Siddiqui, "Methane emission models – a review," *International Journal of Environmental Studies,* 2021.

[49] S. Towprayoon, S. Kim, E.-C. Jeon, T. Ishigaki and S. N. Amadou, "2019 Refinement to the 2006 IPCC Guidelines for National Greenhouse Gas Inventories Chapter 5: Incineration and Open Burning of Waste," Intergovernmental Panel on Climate Change (IPCC), 2019.

[50] American National Standards Institute (ANSI), "ANSI/APA PRG 320-2019 Standard for Performance-Rated Cross-Laminated Timber," APA - The Engineered Wood Association, Tacoma, WA, USA, 2019.

[51] International Standards Organization (ISO), "ISO 14044 Environmental management - Life cycle assessment - Requirements and guidelines," 2006.

[52] I. S. Alemdag, "Mass Equations and Merchantability Factors for Ontario Softwoods Information Report PI-X-23," Petawawa National Forestry Institute, Canadian Forestry Service, Environment Canada, Chalk River, Ontario, Canada, 1983.

[53] City of Portland, "How to Measure a Tree," Portland.gov, [Online]. Available: https://www.portland.gov/trees/tree-care-and-resources/how-measure-tree.

[54] UL Environment, "Product Category Rules for Building-Related Products and Services Part A: Life Cycle Assessment Calculation Rules and Report Requirements," Institut Bauen und Umwelt e.V. and UL Verification Services, Northbrook, Illinois, USA, 2018.

[55] HydrogenTools, "LOWER AND HIGHER HEATING VALUES OF FUELS," Pacific Northwest National Laboratory, [Online]. Available: https://h2tools.org/hyarc/calculator-tools/lower-and-higher-heating-values-fuels.

[56] "Typical calorific values of fuels," Forest Research, [Online]. Available: https://www.forestresearch.gov.uk/tools-and-resources/fthr/biomass-energy-resources/reference-biomass/facts-figures/typical-calorific-values-of-fuels/.

[57] "Fuels - Higher and Lower Calorific Values," Engineering ToolBox, 2003. [Online]. Available: https://www.engineeringtoolbox.com/fuels-higher-calorific-values-d_169.html.

[58] B. Günther, K. Gebauer, R. Barkowski, M. Rosenthal and C.-T. Bues, "Calorific value of selected wood species and wood products," *European Journal of Wood and Wood Products*, vol. 70, no. 5, pp. 755-757, 2012.

[59] N. Krajnc, "Wood Fuels Handbook," FOOD AND AGRICULTURE ORGANIZATION OF THE UNITED NATIONS (FAO), Pristina, Kosovo, 2015.

[60] Athena Sustainable Materials Institute, "A Cradle-to-Gate Life Cycle Assessment of Canadian Glulam," 2018.

[61] T. Bowers, M. E. Puettmann, I. Ganguly and I. Eastin, "Cradle-to-Gate Life-Cycle Impact Analysis of Glued-Laminated (Glulam) Timber: Environmental Impacts from Glulam Produced in the US Pacific Northwest and Southeast," *Forest Products Journal*, vol. 67, no. 5/6, pp. 368-380, 2017.

[62] M. Puettmann, E. Oneil and L. Johnson, "Cradle to Gate Life Cycle Assessment of Glue Laminated Timbers Production from the Pacific Northwest," 2013.

[63] M. E. Puettmann and J. B. Wilson, "GATE-TO-GATE LIFE-CYCLE INVENTORY OF GLUED-LAMINATED TIMBERS PRODUCTION," *Wood and Fiber Science,* no. 37 Corrim Special Issue, pp. 99-113, 2005.

Appendix A AGTP Factors for Unit Emissions and Sequestrations

The tables provided in this Appendix provide AGTP factors for unit (1 kg) emissions and sequestrations, AGTP, of CO_2 and CH_4. Values are in units of 10^{-6} nanokelvins (nK), where 1 nK = 10^{-9} K. The leftmost column 'Time Horizon (Years)' in all tables refers not to the overall assessment time horizon of the LCA study, but to the time difference between the initiation of the emission event and the assessment time horizon. If an emission event, such as forest growth, initiates at year 0 (the year of building construction), then the 'Time Horizon' used to select an AGTP factor is the assessment time horizon. However, if the event initiates at any other time, then the 'Time Horizon' used should be the assessment time horizon minus the time of initiation. For example, if the assessment time horizon is 100 years and end-of-life emissions from waste treatment initiate in year 60, then the 'Time Horizon' used to select an AGTP factor for waste treatment emissions should be 100 - 60 = 40 years.*

Table 2: Absolute Global Temperature Change Potentials AGTP* for 1 kg CO_2 and CH_4 emissions distributed following the delta function, e(t) = δ(t) (i.e. pulse emissions).

Time Horizon (Years)	AGTP (CO_2)	AGTP (CH_4)	Time Horizon (Years)	AGTP (CO_2)	AGTP (CH_4)
2	0.219	17.289	65	0.523	2.485
4	0.357	27.602	70	0.516	2.121
6	0.455	33.603	75	0.509	1.870
8	0.526	36.538	80	0.504	1.697
10	0.576	37.336	85	0.499	1.577
12	0.610	36.685	90	0.495	1.491
14	0.632	35.092	95	0.491	1.429
16	0.646	32.924	100	0.487	1.382
18	0.652	30.446	110	0.481	1.317
20	0.654	27.842	120	0.476	1.272
25	0.645	21.520	130	0.471	1.235
30	0.627	16.138	140	0.467	1.203
35	0.607	11.926	150	0.463	1.173
40	0.587	8.787	160	0.459	1.144
45	0.570	6.518	170	0.456	1.116
50	0.555	4.912	180	0.452	1.089
55	0.543	3.792	190	0.449	1.063
60	0.532	3.017	200	0.446	1.037

Table 3: Absolute Global Temperature Change Potentials AGTP* for 1 kg CO_2 emissions distributed following the negative exponential function, $e(t) = (1/\tau)e^{-t/\tau}$.

Time Horizon (Years)	Characteristic (e-folding) Time, τ (years)									
	5	10	15	20	25	30	35	40	45	50
2	0.045	0.024	0.017	0.013	0.010	0.008	0.007	0.006	0.006	0.005
4	0.130	0.074	0.052	0.040	0.032	0.027	0.023	0.020	0.018	0.017
6	0.225	0.136	0.097	0.075	0.061	0.052	0.045	0.040	0.035	0.032
8	0.316	0.201	0.147	0.115	0.095	0.080	0.070	0.062	0.055	0.050
10	0.397	0.266	0.198	0.157	0.130	0.111	0.097	0.086	0.077	0.070
12	0.465	0.326	0.248	0.199	0.166	0.142	0.125	0.111	0.100	0.091
14	0.519	0.381	0.295	0.239	0.201	0.173	0.152	0.136	0.122	0.111
16	0.561	0.428	0.338	0.278	0.235	0.204	0.179	0.160	0.145	0.132
18	0.593	0.469	0.377	0.313	0.267	0.232	0.206	0.184	0.167	0.153
20	0.615	0.503	0.412	0.346	0.297	0.260	0.231	0.207	0.188	0.172
25	0.641	0.562	0.480	0.414	0.361	0.320	0.287	0.259	0.237	0.218
30	0.641	0.592	0.525	0.463	0.411	0.369	0.333	0.304	0.279	0.258
35	0.628	0.603	0.551	0.497	0.449	0.407	0.371	0.341	0.314	0.292
40	0.611	0.601	0.565	0.520	0.476	0.436	0.401	0.371	0.344	0.321
45	0.593	0.593	0.569	0.533	0.494	0.458	0.425	0.395	0.369	0.345
50	0.576	0.582	0.567	0.540	0.507	0.474	0.443	0.415	0.389	0.366
55	0.562	0.570	0.563	0.542	0.515	0.486	0.457	0.431	0.406	0.384
60	0.549	0.558	0.556	0.541	0.519	0.494	0.468	0.443	0.420	0.398
65	0.538	0.547	0.548	0.538	0.521	0.499	0.476	0.453	0.431	0.411
70	0.529	0.537	0.540	0.534	0.521	0.502	0.482	0.461	0.441	0.421
75	0.521	0.528	0.533	0.530	0.519	0.504	0.486	0.467	0.448	0.430
80	0.515	0.520	0.526	0.525	0.517	0.504	0.489	0.472	0.454	0.437
85	0.509	0.514	0.519	0.520	0.514	0.504	0.491	0.475	0.459	0.443
90	0.504	0.508	0.513	0.515	0.511	0.503	0.491	0.478	0.463	0.448
95	0.500	0.503	0.508	0.510	0.508	0.502	0.492	0.480	0.466	0.453
100	0.496	0.498	0.503	0.506	0.505	0.500	0.491	0.481	0.469	0.456
110	0.489	0.491	0.494	0.498	0.498	0.495	0.490	0.482	0.472	0.461
120	0.483	0.484	0.487	0.490	0.492	0.491	0.487	0.481	0.473	0.464
130	0.478	0.479	0.481	0.484	0.486	0.486	0.484	0.479	0.473	0.466
140	0.474	0.474	0.476	0.479	0.481	0.481	0.480	0.477	0.473	0.467
150	0.469	0.469	0.471	0.474	0.476	0.477	0.477	0.475	0.471	0.466
160	0.466	0.465	0.467	0.469	0.471	0.473	0.473	0.472	0.469	0.465
170	0.462	0.462	0.463	0.465	0.467	0.468	0.469	0.469	0.467	0.464
180	0.459	0.458	0.459	0.461	0.463	0.465	0.465	0.465	0.464	0.462
190	0.455	0.455	0.456	0.457	0.459	0.461	0.462	0.462	0.462	0.460
200	0.452	0.452	0.453	0.454	0.456	0.457	0.459	0.459	0.459	0.458

Table 4: Absolute Global Temperature Change Potentials AGTP* for 1 kg CH_4 emissions distributed following the negative exponential function, $e(t) = (1/\tau)e^{-t/\tau}$.

Time Horizon (Years)	Characteristic (e-folding) Time, τ (years)									
	5	10	15	20	25	30	35	40	45	50
2	3.565	1.903	1.297	0.984	0.793	0.663	0.571	0.500	0.446	0.402
4	10.201	5.801	4.045	3.104	2.518	2.118	1.828	1.607	1.434	1.295
6	17.243	10.425	7.438	5.776	4.720	3.990	3.455	3.046	2.724	2.464
8	23.363	14.985	10.942	8.602	7.082	6.017	5.230	4.625	4.145	3.755
10	28.024	19.030	14.224	11.323	9.396	8.027	7.004	6.211	5.580	5.064
12	31.128	22.335	17.093	13.784	11.531	9.905	8.678	7.720	6.951	6.322
14	32.805	24.824	19.454	15.897	13.410	11.585	10.192	9.096	8.212	7.483
16	33.284	26.509	21.280	17.625	14.996	13.033	11.516	10.312	9.333	8.523
18	32.819	27.461	22.583	18.964	16.280	14.235	12.636	11.354	10.304	9.431
20	31.655	27.773	23.403	19.932	17.267	15.195	13.551	12.219	11.122	10.202
25	26.998	26.456	23.705	20.941	18.580	16.626	15.012	13.666	12.532	11.566
30	21.578	23.345	22.256	20.427	18.588	16.935	15.495	14.251	13.175	12.241
35	16.590	19.585	19.866	18.970	17.730	16.463	15.278	14.206	13.249	12.396
40	12.481	15.879	17.123	17.031	16.367	15.504	14.605	13.738	12.931	12.190
45	9.305	12.586	14.404	14.931	14.768	14.283	13.666	13.011	12.365	11.749
50	6.948	9.842	11.915	12.874	13.112	12.956	12.597	12.145	11.658	11.168
55	5.248	7.655	9.754	10.976	11.514	11.627	11.493	11.224	10.885	10.514
60	4.044	5.964	7.942	9.293	10.037	10.359	10.411	10.301	10.094	9.834
65	3.203	4.688	6.463	7.840	8.712	9.187	9.388	9.411	9.320	9.158
70	2.620	3.742	5.279	6.611	7.547	8.128	8.443	8.574	8.580	8.504
75	2.218	3.051	4.345	5.588	6.539	7.185	7.583	7.800	7.887	7.884
80	1.942	2.550	3.617	4.745	5.676	6.354	6.810	7.092	7.244	7.303
85	1.750	2.190	3.055	4.057	4.943	5.630	6.121	6.450	6.654	6.763
90	1.617	1.932	2.624	3.499	4.325	5.001	5.510	5.872	6.115	6.265
95	1.522	1.747	2.294	3.048	3.805	4.457	4.971	5.354	5.626	5.808
100	1.454	1.614	2.043	2.685	3.371	3.989	4.496	4.890	5.182	5.389
110	1.365	1.447	1.705	2.159	2.704	3.240	3.714	4.106	4.418	4.656
120	1.308	1.352	1.506	1.819	2.239	2.688	3.112	3.484	3.795	4.047
130	1.266	1.291	1.384	1.597	1.914	2.282	2.651	2.991	3.289	3.541
140	1.231	1.248	1.305	1.449	1.686	1.981	2.295	2.599	2.877	3.120
150	1.200	1.212	1.249	1.347	1.522	1.756	2.020	2.287	2.540	2.770
160	1.170	1.180	1.206	1.273	1.402	1.587	1.806	2.038	2.265	2.478
170	1.141	1.151	1.170	1.218	1.313	1.458	1.638	1.837	2.039	2.234
180	1.114	1.122	1.138	1.173	1.244	1.357	1.505	1.675	1.853	2.029
190	1.087	1.095	1.109	1.135	1.189	1.278	1.399	1.542	1.698	1.856
200	1.061	1.069	1.081	1.102	1.144	1.214	1.312	1.434	1.569	1.710

Table 5: Absolute Global Temperature Change Potentials AGTP* for 1 kg CO_2 sequestrations distributed following the Schnute growth function [28], $e(t) = (a/b)e^{-at}(1-e^{-at})^{(1-b)/b}$.

Time Horizon (Years)	Forest Rotation Period, *r* (years)							
	25	50	75	100	125	150	175	200
2	-0.001	0.000	0.000	0.000	0.000	0.000	0.000	0.000
4	-0.014	-0.001	0.000	0.000	0.000	0.000	0.000	0.000
6	-0.055	-0.007	-0.002	-0.001	0.000	0.000	0.000	0.000
8	-0.125	-0.023	-0.006	-0.002	-0.001	0.000	0.000	0.000
10	-0.210	-0.050	-0.015	-0.006	-0.003	-0.001	-0.001	0.000
12	-0.298	-0.088	-0.030	-0.012	-0.006	-0.003	-0.002	-0.001
14	-0.380	-0.136	-0.051	-0.022	-0.011	-0.006	-0.003	-0.002
16	-0.450	-0.189	-0.078	-0.036	-0.018	-0.010	-0.006	-0.003
18	-0.508	-0.246	-0.111	-0.053	-0.028	-0.016	-0.009	-0.006
20	-0.552	-0.302	-0.148	-0.075	-0.040	-0.023	-0.014	-0.009
25	-0.618	-0.427	-0.248	-0.142	-0.083	-0.051	-0.032	-0.021
30	-0.639	-0.517	-0.346	-0.219	-0.139	-0.089	-0.059	-0.040
35	-0.635	-0.571	-0.429	-0.297	-0.201	-0.137	-0.094	-0.066
40	-0.620	-0.597	-0.491	-0.367	-0.264	-0.189	-0.135	-0.098
45	-0.602	-0.605	-0.533	-0.426	-0.324	-0.242	-0.180	-0.134
50	-0.584	-0.601	-0.557	-0.471	-0.376	-0.292	-0.225	-0.173
55	-0.568	-0.590	-0.569	-0.503	-0.420	-0.338	-0.268	-0.212
60	-0.554	-0.578	-0.572	-0.525	-0.454	-0.378	-0.309	-0.250
65	-0.541	-0.565	-0.569	-0.538	-0.480	-0.412	-0.346	-0.286
70	-0.531	-0.552	-0.563	-0.544	-0.499	-0.440	-0.378	-0.319
75	-0.522	-0.541	-0.555	-0.546	-0.512	-0.462	-0.405	-0.349
80	-0.515	-0.531	-0.546	-0.544	-0.520	-0.479	-0.428	-0.376
85	-0.509	-0.523	-0.538	-0.541	-0.524	-0.491	-0.447	-0.398
90	-0.503	-0.515	-0.530	-0.536	-0.526	-0.499	-0.462	-0.418
95	-0.498	-0.509	-0.522	-0.530	-0.525	-0.505	-0.473	-0.434
100	-0.494	-0.503	-0.515	-0.524	-0.523	-0.508	-0.482	-0.447
110	-0.487	-0.494	-0.504	-0.513	-0.516	-0.510	-0.492	-0.467
120	-0.481	-0.487	-0.495	-0.503	-0.509	-0.507	-0.497	-0.479
130	-0.475	-0.481	-0.487	-0.495	-0.501	-0.502	-0.497	-0.485
140	-0.471	-0.475	-0.481	-0.487	-0.493	-0.497	-0.495	-0.487
150	-0.466	-0.470	-0.475	-0.481	-0.487	-0.491	-0.491	-0.487
160	-0.462	-0.466	-0.470	-0.475	-0.481	-0.485	-0.487	-0.485
170	-0.459	-0.462	-0.466	-0.470	-0.475	-0.480	-0.483	-0.482
180	-0.455	-0.459	-0.462	-0.466	-0.471	-0.475	-0.478	-0.479
190	-0.452	-0.455	-0.458	-0.462	-0.466	-0.470	-0.474	-0.476
200	-0.449	-0.452	-0.455	-0.458	-0.462	-0.466	-0.470	-0.472

Appendix B Specific LCA Procedure for Mass Timber Buildings

This Appendix detailed a specific version of the proposed LCA method (Figure 14) for mass timber buildings. This formulation may be suitable for inclusion in LCA standards. Note that use stage (modules B1-B7 in standard BS EN 15978:2011 [37]) and end-of-life emissions (modules C1-C7) aside from bioCO_2 emissions from used mass timber components are not included in this procedure. The reason for this was explained in section 4.3.

Table 6: Specific LCA procedure for mass timber buildings.

1. Estimate the building's expected lifetime and select a time horizon for impact assessment.

2. Determine the wet mass of wood contained in the building, M_w, and use it to calculate the CO_2 quantities M_{bld}, M_{tot}, and M_{res} using equations 16, 17, and 18:

$$M_{bld} = 50\% \times \frac{M_w}{1+MC} \times \frac{MW_{CO2}}{MW_C} \quad (16)$$

Where:

- *M_{bld} is the mass of CO_2, in [kg], sequestered in the building's wooden components.*
- *M_w is the wet mass of wood that the building contains, in [kg]. This can be obtained from a material takeoff for the building.*
- *MC is the in-service moisture content of the wooden components. If this information is not available, a value of 15% is recommended based on the requirement by ANSI/APA PRG 320-2019, the North American CLT standard, that the in-service moisture content of CLT panels in Canada shall not exceed 15% over a* year *[50].*
- *MW_{CO2}, MW_C are the molecular weights of CO_2 (44.01 g/mol) and carbon (12.01 g/mol), respectively.*

$$M_{tot} = \frac{M_{bld}}{\eta_{for} \times \eta_{lum} \times \eta_{MT}} \quad (17)$$

Where:

- *M_{tot} is the total mass of CO_2 sequestered by the trees that were felled to produce the building's wooden components, in [kg].*
- *η_{for} is the material efficiency of forest harvest, defined as the oven-dry mass of logs removed from the forest stand divided by the total oven-dry mass of the felled trees, which include residues like branches and stumps left at the harvest site.*
- *η_{lum} is the material efficiency of lumber production in sawmills, defined as the oven-dry mass of sawn lumber produced divided by the oven-dry mass of logs used.*

- *η_{MT} is the material efficiency of the manufacturing of mass timber components like CLT panels and glulam beams. It is defined as the oven-dry mass of mass timber components produced by the manufacturing plant divided by the oven-dry mass of the sawn lumber used. Recommended values for all three material efficiencies are discussed in Appendix D.*

$$M_{res} = M_{tot} - M_{bld} \quad (18)$$

Where:

- *M_{res} is the mass of CO_2 contained in woody residues that do not become part of the finished building, including:*
  - *From forest harvest: tree tops, branches, foliage, and stumps.*
  - *From lumber production: bark, sawdust, wood chips, and slabs and edgings not large enough to become lumber.*
  - *From mass timber component manufacturing: sawdust, wood chips, and trimmings (e.g. cut-outs from CLT panels for windows and doors).*

3. Calculate the AGTP contribution by emissions incurred during the manufacturing, transport, and construction (MTC) stages, $AGTP_{MTC}$.

Notes:

- *These stages are given by modules A1-A5 in standard BS EN 15978:2011 [37].*
- *MTC emissions include those associated with both wood and non-wood components of the building, such as foundations, windows, cladding, etc.*
- *The principal gas emitted from the MTC stages shall be assumed to be CO_2.*
- *MTC emissions shall be modeled as a pulse emission occurring at year 0 using the delta function $\delta(t)$.*

3.1	Determine the total quantity of CO_2 emitted during the MTC stages, M_{MTC}, using conventional life cycle inventory (LCI) accounting methods. ● *Emissions associated with non-wood materials can be obtained from environmental product declarations, and emissions from transportation can be calculated based on distances from manufacturing facilities to the construction site and emission intensities of the transportation modes used.* ● *Guidance on LCI analysis is provided in section 4.3 of ISO 14044:2006 [51] and section 7.2 of ISO 21930:2017 [22].*
3.2	Using Table 2 in Appendix A, determine the AGTP of a 1 kg pulse emission of CO_2 from the MTC stages, $AGTP^*_{MTC}$, based on the assessment time horizon.

3.3	Compute the total AGTP contribution by the MTC stages, $AGTP_{MTC}$, by multiplying M_{MTC} by $AGTP^*_{MTC}$ (equation 19). $AGTP_{MTC} = M_{MTC} \times AGTP^*_{MTC}$ (19)
4. Calculate the AGTP contribution by treatment of forest, sawmill, and mass timber manufacturing residues, $AGTP_{res}$.	
4.1	Determine the treatment methods used for the residues. If multiple treatment methods are used, then for each method *i*, determine the fraction of M_{res} that it accounts for. Note that all fractions must sum to 1. ● *For residues that are re-manufactured into other long-lived products (e.g. particle board or insulation materials) that are expected to last beyond the assessment time horizon, their impacts can be ignored from the assessment.*
4.2	For each treatment method *i*, determine the principal greenhouse gas emitted and the total amount released, M_i.
4.3	For each treatment method *i*, select an emission function $e_i(t)$ that best represents how emissions arising from it are distributed over time. ● *For the treatment method "incineration", the recommended emission function is the delta function $\delta(t)$.* ● *For the treatment method "aerobic decay", the recommended emission function is the negative exponential function $e_i(t) = (1/\tau)e^{-t/\tau}$ with $\tau = 10$ years (explained in section 4.5.2).* ● *For residues that are re-manufactured into short-lived products (e.g. paper) that are not expected to last beyond the assessment time horizon, model their emissions as pulses (using the delta function) occurring at the expected lifetimes of the products.*
4.4	For each treatment method *i*, using the tables provided in Appendix A, determine the AGTP of 1 kg of the emitted gas, $AGTP^*_i$, based on the gas emitted, the emission function $e_i(t)$, and the assessment time horizon.
4.5	Compute the total AGTP contribution by residue treatment, $AGTP_{res}$, using equation 20: $AGTP_{res} = \sum_{i=1}^{n} M_i \times AGTP^*_i$ (20)
5. Calculate the AGTP contribution by waste treatment of used mass timber building components at the building's end-of-life stage, $AGTP_{bld}$.	

5.1	Determine the treatment method used for the end-of-life building components. If multiple treatment methods are used, then for each method *j*, determine the fraction of M_{bld} that it accounts for. Note that all fractions must sum to 1. ● *For components that are reused or recycled into other long-lived products that are expected to last beyond the assessment time horizon, their impacts can be ignored from the assessment.*
5.2	For each treatment method *j*, determine the principal greenhouse gas emitted and the total amount released, M_j. *Equation 21 below can be used to calculate the total quantity of methane (CH4) released from landfill decomposition of mass timber components.* $M_{CH4} = 0.019 \times 50\% \times \frac{M_{w,landfill}}{1+MC} \times \frac{MW_{CH4}}{MW_C}$ (21) *Where:* ● *0.019 is the methane potential of wood provided by Micales and Skog (1997) [33], defined as the fraction of carbon contained in the landfilled wood that is eventually released as CH_4.* ● $M_{w,landfill}$ *is the wet mass of mass timber components, in [kg], sent to landfill.* ● *MC is the in-service moisture content of the mass timber components. Like in step 2, if this information is not available, a value of 15% is recommended based on ANSI/APA PRG 320-2019 [50].* ● MW_{CH4}, MW_C *are the molecular weights of CH_4 (16.04 g/mol) and carbon (12.01 g/mol), respectively.*
5.3	For each treatment method *j*, select an emission function $e_j(t)$ that best represents how emissions arising from it are distributed over time. ● *For the treatment method "incineration", the recommended emission function is the delta function $\delta(t)$.* ● *For the treatment method "landfill decay", the recommended emission function is the negative exponential function $e_i(t) = (1/\tau)e^{-t/\tau}$ with $\tau = 43.3$ years (explained in section 4.5.2)* ● *For components that are re-manufactured into short-lived products that are not expected to last beyond the assessment time horizon, model their emissions as pulses (using the delta function) occurring at the expected lifetimes of the products.*

5.4	For each treatment method *j*, using the tables provided in Appendix A, determine the AGTP of 1 kg of the emitted gas, $AGTP^*_j$, based on the gas emitted, the emission function $e_j(t)$, and the assessment time horizon. ● *Since end-of-life emissions do not begin at year 0, when using Appendix A to select $AGTP^*_j$ values, the time horizon used shall be equal to the assessment time horizon minus the building's expected lifetime. For instance, if the assessment time horizon is 100 years and the building's lifetime is 60 years, then the time horizon used for selecting $AGTP^*_j$ is 100 - 60 = 40 years.*
5.5	Compute the total AGTP contribution by end-of-life waste treatment of used mass timber components, $AGTP_{bld}$, using equation 22: $AGTP_{bld} = \sum_{j=1}^{n} M_j \times AGTP^*_j$ (22)
6. Calculate the reduction in AGTP associated with carbon sequestration by forest growth, $AGTP_{for}$. *Note: AGTP reduction by forest growth can only be claimed if it can be proven that the forest stand has a very high likelihood of regenerating to pre-harvest conditions.*	
6.1	Determine the rotation period of the forest stand from which the wood used in the building was extracted.
6.2	Using Table 5 in Appendix A, determine the AGTP of 1 kg of CO_2 sequestered by forest regrowth, $AGTP^*_{for}$, based on the forest rotation period and the assessment time horizon.
6.3	Calculate the AGTP reduction by forest regrowth using equation 23 below. $AGTP_{for} = M_{tot} \times AGTP^*_{for}$ (23)
7. Calculate the total AGTP of the building at the chosen assessment time horizon by summing the contributions by emissions from MTC, residue treatment, end-of-life waste treatment, and forest regrowth. $AGTP_{tot} = AGTP_{MTC} + AGTP_{res} + AGTP_{bld} + AGTP_{for}$ (24)	

Appendix C Sample Calculation Using the Proposed LCA Method

In this Appendix, the LCA method outlined in Appendix B is used to calculate the AGTP of the analysis scenario with a 78-year assessment time horizon and a 75-year forest rotation period.

1. Estimate the building's expected lifetime and select a time horizon for impact assessment.

As discussed in section 4.5.1, the case study building's lifetime is assumed to be 60 years. The assessment time horizon for this analysis scenario is 75 years.

2. Determine the wet mass of wood contained in the building, M_w, and use it to calculate the CO_2 quantities M_{bld}, M_{tot}, and M_{res}.

The original study by Chen et al. (2020) [35] provided that the mass of wood contained in the case study building, on a wet basis, is 1.1382×10^6 kg. In a real world LCA study, this quantity would be obtained from a material takeoff for the building. The wood is assumed to have a moisture content of 12%, consistent with the original study. Thus, using equation 16, the mass of CO_2 sequestered in the building's wooden component is:

$$M_{bld} = 50\% \times \frac{1{,}138{,}200\ kg}{1 + 0.12} \times \frac{44.01\ g/mol}{12.01\ g/mol} = 1.862 \times 10^6\ kg$$

The material efficiencies of forest harvest, lumber production, and mass timber manufacturing, defined in Appendix B, are taken to be 72.35%, 75.88%, and 84.97%, respectively. The derivations of these values are discussed in Appendix D. Substituting these into equation 17, the total mass of CO_2 sequestered in the trees harvested is:

$$M_{tot} = \frac{1.862{,}000\ kg}{0.7235 \times 0.7588 \times 0.8497} = 3.992 \times 10^6\ kg$$

Finally, substituting M_{bld} and M_{tot} into equation 18, the mass of CO_2 contained in the residues resulting from forest harvest, lumber production, and mass timber manufacturing is:

$$M_{res} = 3.992 \times 10^6\ kg - 1.862 \times 10^6\ kg = 2.129 \times 10^6\ kg$$

3. Calculate the AGTP contribution by emissions incurred during the manufacturing, transport, and construction (MTC) stages, $AGTP_{MTC}$.

As given by the original study [35], the total amount of CO_2 emitted in stages A1-A5 is 1.526×10^6 kg. This includes emissions associated with non-wood components such as the building's concrete foundation. Using Table 2 in Appendix A, by linear interpolation, the AGTP of a 1 kg pulse CO_2 emission at a 78-year time horizon, $AGTP^*_{MTC}$, is 0.5058×10^{-6} nK. Knowing this information, the AGTP contribution by MTC emissions is:

$$AGTP_{MTC} = 1.526 \times 10^6\ kg \times 0.5058 \times 10^{-6}\ nK/kg = 0.772\ nK$$

4. Calculate the AGTP contribution by treatment of forest, sawmill, and mass timber manufacturing residues, $AGTP_{res}$.

As mentioned in section 4.5.2, it is assumed that 2 treatment methods are used for residues:

1. Incineration (50% of M_{res}), and
2. Aerobic decomposition (the remaining 50%).

As incineration releases CO_2 as a pulse, the AGTP for a 1 kg emission at a 78-year time horizon, $AGTP^*_1$, is also 0.5058×10^{-6} nK. Referring again to section 4.5.2, emissions from aerobic decomposition are modeled using a negative exponential function with characteristic time $\tau = 10$ years. Thus, using Table 3, by linear interpolation, $AGTP^*_2$ is 0.5234×10^{-6} nK. The AGTP contribution by residue treatment can then be found:

$$AGTP_{res} = \sum_{i=1}^{2} M_i \times AGTP^*{}_i = (M_1 \times AGTP^*{}_1) + (M_2 \times AGTP^*{}_2)$$

$$AGTP_{res} = \left(\frac{2.129 \times 10^6\ kg}{2} \times 0.5058 \times 10^{-6}\ nK/kg\right) + \left(\frac{2.129 \times 10^6\ kg}{2} \times 0.5234 \times 10^{-6}\ nK/kg\right) = 1.096\ nK$$

5. Calculate the AGTP contribution by waste treatment of used mass timber building components at the building's end-of-life stage, $AGTP_{bld}$.

As discussed in section 4.5.2, it is assumed that 2 treatment methods are used for end-of-life mass timber components:

1. Incineration (50% of M_{bld}), and
2. Landfill (the remaining 50%).

Since the building's end-of-life stage occurs at year 60, which is only 18 years away from the assessment time horizon, a time horizon of 18 years is used when selecting $AGTP^*_j$ for the two treatment methods. Incineration, again, releases CO_2 as a pulse. From Table 2, using a time horizon of 18 years, $AGTP^*_1$ is 0.6522×10^{-6} nK. The principal gas emitted from landfill is methane, and the emissions can be modeled using a negative exponential function with a characteristic decay time τ of 43.3 years [33] [49] (see section 4.5.2). Thus, by linear interpolation using Table 4, $AGTP^*_2$ is 10.665×10^{-6} nK. The AGTP contribution by end-of-life treatment can be then calculated:

$$AGTP_{bld} = \sum_{j=1}^{2} M_j \times AGTP^*_j = (M_1 \times AGTP^*_1) + (M_2 \times AGTP^*_2)$$

$$M_2 = M_{CH4} = 0.019 \times \frac{M_{bld}}{2} \times \frac{MW_{CH4}}{MW_{CO2}} = 0.019 \times \frac{1.862 \times 10^6\ kg}{2} \times \frac{16.04}{44.01} = 6447\ kg$$

$$AGTP_{bld} = (\frac{1.862 \times 10^6\ kg}{2} \times 0.6522 \times 10^{-6}\ nK/kg) + (6447\ kg \times 10.665 \times 10^{-6}\ nK/kg)$$

$$AGTP_{bld} = 0.676\ nK$$

6. Calculate the reduction in AGTP associated with carbon sequestration by forest growth, $AGTP_{for}$.

Given a forest rotation period of 75 years and a time horizon of 78 years, using Table 5, $AGTP^*_{for}$ is -0.5497×10^{-6} nK. The AGTP reduction due to forest regrowth is thus:

$$AGTP_{for} = 3.992 \times 10^6\ kg \times -0.5497 \times 10^{-6}\ nK/kg = -2.194\ nK$$

7. Calculate the total AGTP of the building at the chosen assessment time horizon by summing the contributions by MTC emissions, residue treatment, end-of-life waste treatment, and forest regrowth.

Finally, adding together the results of the previous steps gives:

$$AGTP_{tot} = AGTP_{MTC} + AGTP_{res} + AGTP_{bld} + AGTP_{for}$$

$$AGTP_{tot} = 0.772\ nK + 1.096\ nK + 0.676\ nK - 2.194\ nK = 0.350\ nK$$

In conclusion, the global surface temperature impact of the case study building 78 years after its construction, assuming a forest rotation period of 75 years, is 0.35 nanokelvins.

Appendix D Derivation of Material Efficiencies

In Appendix C, when calculating the total mass of CO_2 sequestered by forest growth using equation 17, the material efficiencies of forest harvest (η_{for}), lumber production (η_{lum}), and mass timber manufacturing (η_{MT}), were assumed to be 72.35%, 75.88%, and 84.97%, respectively. This Appendix discusses how these values were determined.

1. Material efficiency of forest harvest, η_{for}

The material efficiency of forest harvest, defined in Appendix B as the ovendry mass of logs removed from the forest stand divided by the total ovendry mass of the felled trees, was estimated using an Environmental Canada publication (Alemdag (1983) [52]). This paper provided equations for estimating the ovendry masses of various components of softwood trees in Ontario, as well as merchantable fractions of a tree stem. According to it, the ovendry mass (OM), in kilograms, of the whole tree or any fraction of it (e.g. stem wood, stem bark, branches, etc.) can be estimated using the following equation:

$$OM = b_1 \cdot d^2 h \tag{25}$$

Where:

- b_1 is a proportionality constant whose value depends on tree species the fraction for which the ovendry mass is desired,
- d is the tree's diameter at breast height, in [cm], which is its diameter measured 4.5 feet above the ground [53], and
- h is the total height of the tree, in [m].

Additionally, the percentage of the OM of the tree stem that is merchantable as wood or bark, as well as the mass of the unmerchantable tree top as a percentage of the ovendry stem mass, can be estimated using the following equation:

$$OM\% = b_0 + b_1 \cdot (dm/d) + b_2 \cdot (dm/d)^2 \tag{26}$$

Where:

- b_0, b_1, and b_2 are parameters that depend on tree species and the component of interest,

- dm is the tree's 'merchantable top diameter outside bark', which is the diameter of the stem at the height above which the tree is no longer considered merchantable, and
- d, again, is the tree' diameter at breast height, in [cm].

The above two models were validated by [52] using empirical data, which found high coefficients of determination (r^2). The paper provided field data collected for various softwood tree species in Ontario, which was input into the above equations to estimate the average material efficiency associated with forest harvesting. Out of 722 trees for which data was collected, the average diameter at breast height was d = 24.6 cm, and the average total tree height was 17.13 m. Given this information, using equation 25 above, the OM of various tree components as well as of the average softwood tree can be calculated, as shown in Table 7 below. For example, the average OM of stem wood in a tree (coefficient b_1 = 0.011718, as provided by [52]) is:

$$OM_{stem\,wood} = 0.011718 \cdot (24.6)^2(17.13) = 121.5\ kg$$

Table 7: Estimating the average OM of a softwood tree using Alemdag (1983)'s [52] model.

Tree Component	**b_1**	**OM (kg)**
Stem wood	0.011718	121.47
Stem bark	0.001580	16.38
Live branches	0.002393	24.81
Twigs plus needles	0.000918	9.52
Dead branches	0.000437	4.53
Stem total (wood + bark)	n/a	137.85
Tree total (all components)	n/a	176.71

The study also provided coefficients b_0, b_1, and b_2 for use in equation 26 for computing quantities of merchantable stem wood and merchantable stem bark as percentages of the OM of the tree stem. The merchantable top diameter dm used is 9.1 cm as the study [52] seems to suggest that this is the smallest possible diameter of a merchantable log. Given an average diameter at breast height of 24.6 cm, the ratio dm/d is 9.1/24.6 = 0.37. Using equation 26, the average merchantable percentage of a tree stem can then be estimated, as follows:

$$OM\%_{stem\,wood} = 75.405 + 81.546(0.37) - 132.194(0.37)^2 = 87.48\%$$

$$OM\%_{stem\ bark} = 12.043 + 1.422(0.37) - 9.824(0.37)^2 = 11.22\%$$
$$OM\%_{stem\ total} = OM\%_{stem\ wood} + OM\%_{stem\ bark} = 98.70\%$$

This estimation indicates that on average, 98.7% of the OM of a tree stem can be harvested to be sold. Although this figure seems too high from intuition, it is used nonetheless due to a lack of field data for validation. However, this merchantable percentage includes the tree stump [52], which, despite being considered merchantable, is not removed from the harvest site. Alemdag (1983) [52] found that for an average softwood tree, assuming a stump height of 30 cm, the stump makes up approximately 5.97% of the total stem mass. Thus, the actual mass percentage of a tree stem that is expected to be removed from the harvest site as logs is:

$$OM\%_{stem\ total} = 98.70\% - 5.97\% = 92.73\%$$

Finally, the average material efficiency of forest harvest can be estimated by multiplying $OM\%_{stem\ total}$ by the average OM of a softwood tree stem, 137.85 kg from Table 7 above, and then dividing by the average total OM of a softwood tree, 176.71 kg.

$$\eta_{for} = \frac{OM\%_{stem\ total} \times OM_{stem}}{OM_{tree\ total}} = \frac{92.73\% \times 137.85\ kg}{176.71\ kg} \times 100\% = 72.35\%$$

A limitation of this material efficiency value is that it was computed for softwood trees in Ontario. The material efficiencies associated with other tree species like hardwoods or for forests in other timber-producing regions may be different. However, based on the prescriptive CLT grades and layups provided by ANSI/APA PRG 320-2019 [50], it appears that softwood species like spruce, pine, fir, douglas-fir, and larch are commonly used for mass timber. The calculated material efficiency should thus be acceptable for use in most LCAs of mass timber buildings in North America. Another notable limitation of Alemdag (1983)'s [52] model is that it does not account for the mass of a tree's roots, which may also contain a significant quantity of sequestered CO_2. Thus, the material efficiency of 72.35% is likely an overestimate both because the 98.7% figure for the merchantability of a tree stem seems too high, and because this material efficiency only applies to the aboveground portion of a tree. Refinement of this figure by future research is strongly recommended.

2. Material efficiency of lumber production, η_{lum}

The material efficiency of lumber production, defined in Appendix B as the ovendry mass of lumber produced by a sawmill divided by the ovendry mass of logs input into it, was determined from the 2020 Environmental Product Declaration (EPD) for North American Softwood Lumber [46]. The EPD provides that the amount of 'renewable primary resources with energy content used as material', RPR_M, used to produce 1 m^3 of softwood lumber is 10959.1 MJ. 'Renewable primary resources' is interpreted as referring to the logs from which the softwood lumber is produced. According to Part A of UL's Product Category Rules for Building-Related Products and Services [54], RPR_M is calculated by multiplying the mass of the material used with its lower calorific value (LHV). From several sources ([55], [56], [57], [58], and [59]), the average LHV of oven-dry wood was found to be 18.07 MJ/kg. Thus, the oven-dry mass of logs used to produce 1 m^3 of softwood lumber is approximately:

$$OM_{logs} = \frac{RPR_M}{LHV_{wood}} = \frac{10959.1\ MJ}{18.07\ MJ/kg} = 606.48\ kg$$

According to the EPD [46], the ovendry mass of 1 m^3 of softwood lumber is 460.18 kg. Knowing this, the average material efficiency of lumber production can be estimated:

$$\eta_{lum} = \frac{OM_{lumber}}{OM_{logs}} \times 100\% = \frac{460.18\ kg}{606.48\ kg} \times 100\% = 75.88\%$$

Like with the material efficiency of forest harvest, a limitation of the above value is that it only applies to softwood lumber produced in North America. However, since it appears from ANSI/APA PRG 320-2019 [50] that softwoods are frequently used for mass timber, this value should be acceptable for LCA studies of mass timber buildings in North America.

3. Material efficiency of mass timber manufacturing, η_{MT}

The material efficiency of mass timber manufacturing was defined in Appendix B as the OM of mass timber components produced divided by the OM of the sawn lumber used to produce them. It was determined using 10 LCA studies on CLT and glulam produced in North America, where for each study, the OM of the output product was divided by the OM of the lumber input. For example, according to a 2013 LCA study by the Athena Sustainable Material Institute on

Canadian CLT [8], the ovendry density of CLT is 417.03 kg/m^3, and the OM of the lumber used to produce 1 m^3 of CLT is 477.76 kg. Thus, the material efficiency from this study is:

$$\eta_{MT} = \frac{\rho_{OD,CLT} \times 1\ m^3}{OM_{lumber}} = \frac{417.03\ kg/m^3 \times 1\ m^3}{477.76\ kg} = 87.29\%$$

The following table presents the results of the above calculation for all 10 studies. The resulting average material efficiency is η_{MT} = 84.97%. As the standard deviation is only 3.12%, this material efficiency is likely to be highly representative of mass timber products manufactured in North America.

Table 8: Estimating the material efficiency of mass timber manufacturing using LCA studies.

Study	**Product**	**Company/Location**	**Product Density, ρ_{OD} (OD kg/m^3)**	**Lumber input, OM_{lum} (OD kg)**	**$\eta = (\rho_{OD} \times 1\ m^3)/ OM_{lum}$ x 100%**
[8]	CLT	Canadian average	417.03	477.76	87.29%
[9]	CLT	Structurlam, BC	426.05	474.44	89.80%
[7]	CLT	Western Washington	466	563.86	82.64%
[10]	CLT	Oregon	537.23	648.81	82.80%
[60]	Glulam	Canadian average	428	514.41	83.20%
[61]	Glulam	U.S. Pacific northwest	510.7	574.54	88.89%
[61]	Glulam	U.S. Southeast	590	673.66	87.58%
[62]	Glulam	U.S. Pacific northwest	484	573.55	84.39%
[63]	Glulam	U.S. Pacific northwest	483	592	81.59%
[63]	Glulam	U.S. Southeast	551	676	81.51%
				Average:	**84.97%**
				Std. deviation:	**3.12%**

A limitation of this material efficiency value is that although there exist many types of mass timber products such as nail-laminated timber, laminated veneer lumber, and mass plywood panel [5], only LCAs of cross-laminated timber (CLT) and glue-laminated timber (glulam) were used to estimate it. However, these two products typically exist in large quantities in a mass timber building since CLT is used for panel elements like floors and walls, while glulam is used for linear elements like beams and columns. Although it would be beneficial to also compute

material efficiencies for other mass timber products in future studies, the value of 84.97% should be acceptable for LCAs of most mass timber buildings in North America.

In summary, all three material efficiencies determined above should be reasonable for most LCA studies of mass timber buildings in North America. However, as discussed, they were all derived from limited selections of literature and thus have significant uncertainties and limitations. Their values can significantly affect LCA results since they are involved in the calculation of two crucial CO_2 quantities used by the proposed LCA method: the total mass of CO_2 sequestered by tree growth, M_{tot} (equation 17 in Appendix B), and the total mass of residues from forest harvest, lumber production, and mass timber manufacturing, M_{res} (equation 18). Thus, future research to more precisely determine these material efficiencies is strongly recommended.